



UNIVERSITÀ DEGLI STUDI DI PADOVA

DEPARTMENT OF LAND, ENVIRONMENT, AGRICULTURE AND FORESTRY

EVALUATION OF AREAS BURNED IN WILDFIRE AND PRESCRIBED FIRES USING SPECTRAL INDICES AND SAR DATA

Supervisor

Francesco Pirotti

Co-Supervisor

Fillipe Tamiozzo Pereira Torres

Joyce Machado Nunes Romeiro

Academic Year

2020

Contents

Contents	3
Summary	5
Introduction.....	6
Literature Review.....	7
Objectives	9
Hypothesis	9
Methodology.....	10
Study area	10
Data Collection	10
Sampling.....	11
Data Analysis.....	14
SAR	14
Spectral Indices.....	16
Results	18
NDVI	18
NBR	20
SAR	22
SAR and spectral indices comparison	22
Discussion	24
Conclusions.....	25
Bibliography.....	26
Websites.....	29
Appendix	31
Appendix 1	31
Appendix 2	41
Appendix 3	50
Appendix 4	55

Acknowledgement

I would like to express my gratitude to all those who gave me support to complete this thesis.

First of all, to my parents Francisco C. de Souza Romeiro and Adelma A. Machado Nunes do Nascimento, who always supported me and my aspirations to follow my dreams, even if that meant to live far away from them.

To my dear sister, Juliana Machado Nunes Romeiro that has been with me since forever and knows me better than anyone.

To my fiancé, Guilherme Vescovi Nicchio, for helping me in every kind of way during my entire thesis, from my dishes that he washed so I could focus on writing, to the insights we shared on how to analyse my data.

To the best supervisors that I could have had, Francesco Pirotti and Fillipe Tamiozzo Pereira Torres, for the genius ideas and for helping me with every single doubt that I had, always so quickly and so patiently.

To my colleague João Flávio Costa dos Santos for giving me some brilliant ideas.

To all my amazing friends, specially Luigi Honorato and Guilherme Iecker for the nights of laughter where I could put the thesis aside and worry more about the wine.

To the MedFOR and the European Union for financing my studies and therefore, this research.

Thank you all!

Summary

The present research has two main objectives: assessing how Sentinel-1 C-band synthetic aperture radar (SAR) data works for wildfires and prescribed fires, when compared to Landsat data; and also at evaluating if wildfires have similar fire severity when compared to prescribed fires. To assess these issues, the study was conducted in Alto Minho, a subregion of Portugal, using Landsat data to create a multitemporal analysis. For the SAR response to fire events, Sentinel-1 backscatter values were used, and 29 variables were tested in order to see which ones behave more similarly to the spectral indices. For the comparison between prescribed fires and wildfires, the analyses was conducted using Normalized Burn Ratio (NBR) and Normalized Difference Vegetation Index (NDVI). Using visual interpretation to analyse the SAR response, the Normalized Signal Ratio in percentile 90 (NSR p₉₀) seems to work properly for areas covered with grass and small bushes, but it also seems to work best when the fire severity in the area is greater. 95% of the plots analysed by NSR p₉₀ were considered as a good response to fires, when compared to spectral indices. As for the evaluation of wildfires and prescribed fires severity, severity of summer wildfires are significantly different from severity of prescribed fires. Winter/autumn wildfires are not significantly different in terms of severity from prescribed fires.

Introduction

Wildfires are common in many ecosystems, constituting a natural - even vital - component of the ecology of some forests. However, the large-scale fires with high severity and intensity, that have recently been documented, can be highly destructive (Lourenço and Félix, 2019). This culminates in an imbalance between the wildfire occurrences and the recovery of the ecosystem, which leads to an undesirable alteration of the landscape, and its consequent degradation (Alcañiz et al., 2018).

Fire severity is defined by the loss of or change in organic matter in the soil. Ecosystem responses after the fire, such as soil erosion, vegetation regeneration and restoration of community structure, can be linked to this change in organic matter (Keeley, 2009). There are many variables that influence fire severity, including elevation, slope and aspect (Harris & Taylor, 2017; Lentile, Smith, & Shepperd, 2006), weather and climate (Dillon et al., 2011; Arkle et al., 2012), forest structural characteristics, such as tree density and tree diameter (Lentile et al., 2006; Alexander et al., 2006), and also the fire history of the area (Coppoletta, Merriam, & Collins, 2015; Harvey, Donato, & Turner, 2016; Airey Lauvaux, Skinner, & Taylor, 2016). Fire severity can be easily measured, with remote sensing and soil analyses, but the ecosystem response, that is the most valuable factor for forest managers, is way more complex to assess (Keeley, 2009).

Fuel treatments, such as thinning and prescribed fires, are conducted to alter fuel conditions, in an attempt to make wildfires less severe (Reinhardt, Keane, Calkin, & Cohen, 2008). Prescribed burnings are usually conducted in the spring or fall when climate is cooler and moister, and fire spread and size can be easily controlled (Arkle et al., 2012). Prescribed fires conducted under such conditions can reduce severity and modify the spreading of following wildfires (Finney, McHugh, & Grenfell, 2005; Wimberly, Cochrane, Baer, & Kari, 2009; Fulé et al., 2012; Arkle et al., 2012). However, even though it is assumed that prescribed fires are of low severity, studies have shown that in North-western Portugal ten percent of them have an excessive impact on trees and forest floor (P. Fernandes & Botelho, 2004).

It is difficult to map severity levels in large fires using field-based methods, especially in the Mediterranean areas that have complex topography, steep slopes, inaccessible areas and previous heterogeneous vegetation. After a fire, the burning of the vegetation and the changes in soil moisture make the spectrum of the area change, enabling the evaluation of the area using satellite optical images (Escuin, Navarro, & Fernández, 2008). Nowadays, Landsat imagery at 30-m spatial resolution has been widely used for fire severity evaluation at landscape level, and the most common spectral indices used for this purpose have been the Normalized Difference Vegetation Index (NDVI) and the Normalized Burn Ratio (NBR) (Mallinis, Mitsopoulos, & Chrysafi, 2018), with the NBR being shown as much more sensitive than NDVI to the spectral changes produced by fires with a moderate or extreme severity (Escuin et al., 2008).

Although the results from studies that use optical imagery are satisfactory to monitor and evaluate fire severity, there are also limitations regarding these images, such as presence of clouds, smoke and haze, which reduce the observation capability in the visible/infrared domain. Also, the 16 day-revisit time for Landsat can be considered a limitation when the study focuses on monitoring

the area. Apart from that, there can be also confusion of burned areas with dark soils, shaded regions and water bodies (Imperatore et al., 2017).

Sentinel-1 responds to the Earth Observation needs of the European Union (EU) and has two-satellite constellation (1A and 1B) in the same orbiting pattern, offering six day revisit at the equator and working with a C-band Synthetic aperture radar (SAR) (Torres et al., 2012). Sentinel-1 A and Sentinel-1 B were launched on 03 April 2014 and 25 April 2016, respectively (Colson, Petropoulos, & Ferentinos, 2018) and they offer new opportunities for a systematic monitoring, as they are insensible to sunlight-illumination conditions and work with microwave radiation that allows to penetrate clouds (Imperatore et al., 2017).

The use of satellite imagery to classify burn severity is more and more used to study the effects of prescribed burning and wildfires (P. M. Fernandes, 2015), but still there is a lack of studies about how different is the ecosystem responses after the events of prescribed fires and wildfires, specially using spectral indices. Furthermore, the optical imagery have its own important limitations and there is a gap in the literature about the use of SAR to analyse burned areas.

Literature Review

All these variables that help the prediction of fire severity – e.g. topography, weather, and vegetation type - seem to interact with each other in complex ways, and what is true to one area can have the opposite effect on another area. Prescribed fire effectiveness in decreasing the importance of wildfires is dependent on even more variables. Apart from the above mentioned variables, other factors that influence the effectiveness of prescribed fires are treatment longevity, size of treated area, spatial patterns and location of the treated area in relation to subsequent wildfires (P. M. Fernandes, 2015). Prescribed fires have different results of effectiveness depending on the combinations of these factors.

The current evidence suggests that prescribed fires will only have a relevant impact on wildfire extent if a significant part (5–10 %) of the landscape is treated annually, but the lack of resources make it impossible to treat the necessary area of the landscape every year, therefore prescribed burnings do not have concrete effect on wildfire extent (P. M. Fernandes, 2015). Also, Piñol, Beven, & Viegas (2005) evaluated how different degrees of prescribed fires influence the areas affected by wildfires in Northeast Spain and Central Portugal, and they found that every year a fairly constant size of area is burnt, for both prescribed burns and wildfires together, independently of the prescribed fires treatments. Consequently, it seems that even though prescribed burnings are used in an attempt to decrease the total area burnt every year, chances are they will stay relatively the same.

In addition to that P. Fernandes & Botelho (2004) found that, in normal fire weather, 89% of the prescribed fires comply with wildfire protection needs and ecological integrity maintenance, but in extreme fire weather, only 59% of the prescribed burnings would comply with such terms. Furthermore, after prescribed fires conducted from autumn to spring, the fire behaviour varied from barely sustained and patchy burns to high-intensity and nearly crown fires (P. M. Fernandes & Loureiro, 2013).

Most prescribed fires are small, focused on individual stands and as analysis tool, most studies make use of field-based interpretation (i.e. P.

Fernandes & Botelho, 2004; P. M. Fernandes & Loureiro, 2013; Prichard, Peterson, & Jacobson, 2010) or even spatial autoregressive models (Wimberly et al., 2009). However, according to Cruz, Alexander, & Dam (2014) studies using fire modeling systems to assess prescribed fires effectiveness may not be valid because small changes, even smaller than 2.5%, in the estimated moisture content of fine dead fuel, can produce greatly varying results on the predicted fireline intensity, spread of fire and the onset of crown ignition. With such problems in mind and with the advantage of new free sensors, other studies (i.e. Finney et al., 2005; Arkle et al., 2012; Collins, Griffioen, Newell, & Mellor, 2018) have assessed wildfire severity of treated areas using landscape scale remote sensing.

Satellite open data allows a large audience of researchers to test methods for interpreting phenomena impacting the Earth surface. Some studies in the Mediterranean region, have tested the capacity of different indices that combine red and near-infrared regions to distinguish burned areas. NDVI (Normalized Difference Vegetation Index) is one of them and has been one of those most used, with procedures involving uni-temporal (post-fire) and bi-temporal (pre-fire and post-fire difference) point of view (Pereira, 1999); (Chuvieco, Martín, & Palacios, 2002). In the past, NBR (Normalized Burn Ratio) was less used than NDVI due to the lack of availability of data on the mid-infrared region in the sensors used at that time, such as AVHRR and WIFS. With LANDSAT TM/ ETM and mid-infrared region images (band 7 in the TM/ETM sensors), NBR became more used (Escuin et al., 2008).

Even though the most common indices to evaluate fire severity are NDVI and NBR (Escuin et al., 2008; Mallinis et al., 2018), different studies (Chuvieco et al., 2002; Chen et al., 2011; Veraverbeke et al., 2012) try to find new indices that could improve the analyses of this important issue that is wildfires, such as BAI (Burnt Area Index), SAVI (Soil Adjusted Vegetation Index), IFI (integrated forest index), EVI (enhanced vegetation index), and more, but overall, NBR is still being considered the best index to assess the effects of fire (Collins et al., 2018).

Optical and SAR data have complementary characteristics that can be integrated to provide more information to models and methods. The Sentinel 1 C-band SAR data (Torres et al., 2012) and the Sentinel 2 optical multispectral data (Drusch et al., 2012) provide open data in the two realms of SAR and optical. The datasets are also available as products in Google Earth Engine (GEE), an integrated platform designed to empower not only traditional remote sensing scientists but also a wider audience (Gorelick et al., 2017). With the availability of both optical and SAR data free of cost and already pre-processed, the Copernicus datasets represent an optimal and rapid tool for the assessment of forest damages, such as windthrows.

For instance, in their study Imperatore et al., (2017) used Sentinel-1 C-band synthetic aperture radar (SAR) data to investigate if such sensor can detect burned areas in vegetated regions, and concluded that the VH polarization effectively responded to the fire occurrences, decreasing its value after the fire event. Also, Stroppiana et al. (2015) tested the SAR sensor to map the areas likely to be burned using the fuzzy burned area-mapping algorithm that is an integration of the spectral indices and a region-growing algorithm. However, SAR provides a unique opportunity for detecting and assessing burn scars in the landscape, and to the best of our knowledge, only a few studies (Imperatore et

al., 2017; Stroppiana et al. 2015) have addressed the use of SAR data with such objective.

Objectives

Despite all advances related to fire ecology, the evaluation of prescribed burning effectiveness will remain a challenge in most ecosystems, both from the scientist and decision-maker perspectives, especially as climate change will facilitate more extreme fire events (P. M. Fernandes, 2015). Planning and monitoring procedures on prescribed burnings need to be improved in Portugal, as well as in the whole Mediterranean region, in order to overcome the current deficiencies (P. Fernandes & Botelho, 2004). Furthermore, SAR provides a unique opportunity for detecting and assessing burn scars in the landscape and not enough research has been done to assess its functionality for this issue.

Therefore, this study has the objective to evaluate areas burned in wildfire and prescribed fires using Landsat imagery and SAR data. Specifically, the objectives are to:

- (1) assess if wildfires and prescribed fires bring a significant difference in backscatter signal of Sentinel 1.
- (2) evaluate if wildfires have similar fire severity when compared to prescribed fires

Hypothesis

- (1) Assess how Sentinel 1 data work for wildfires and prescribed fires, when compared to Landsat data

H0: Sentinel 1 and Landsat data will have similar responses

- (2) Evaluate if wildfires have similar fire severity when compared to prescribed fires

H0: Regeneration will be faster in prescribed burning areas

Methodology

Study area

The study was conducted in the Northwestern subregion of Portugal called Alto Minho, which covers an area of 221,884 ha, divided by ten municipalities: Arcos de Valdevez, Caminha, Melgaço, Monção, Paredes de Coura, Ponte da Barca, Ponte de Lima, Valença, Viana do Castelo e Vila Nova de Cerveira.

The subregion has a warm-summer Mediterranean climate (Csb) according to Köppen climate classification, with average precipitation ranging from 28.4 mm in July to 228 mm in December, and average temperature from 9.5°C in January to 20.5°C in July. The dry season is between July and August (Figure 1) (IPMA, 2019). The fire season in Portugal takes place between June and September, which corresponds to the warm and dry summer, typical of Mediterranean climates (Pereira, 1999). The study site was chosen due to its specially high fire occurrences (Oliveira et al., 2018), and all areas considered for the analyses of this study were covered by grass and small bushes, belonging to the Genisteeae tribe, which are not used as pasture.

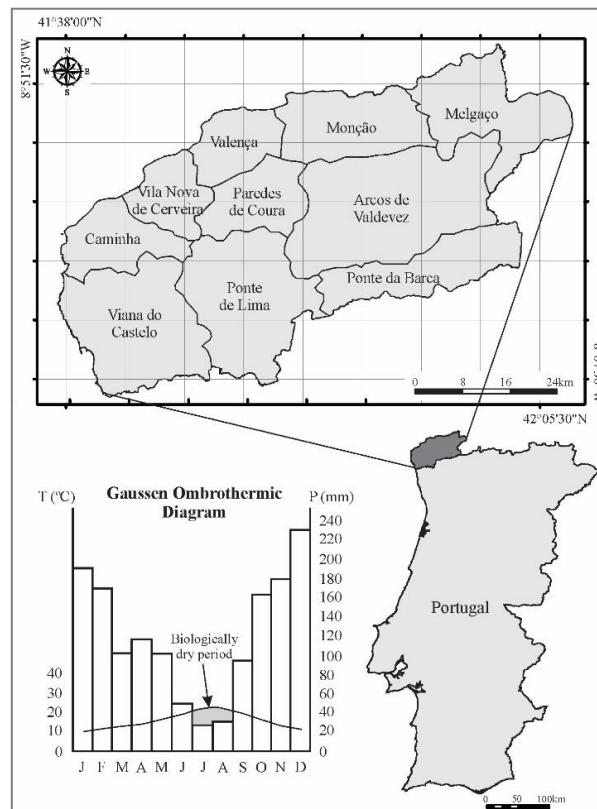


Fig 1. Location and climate of the study area.

Data Collection

Data on wildfire occurrences were collected from the Institute for Nature Conservation and Forests website (ICNF, 2020) in the format of shapefiles containing information on the attribute table such as date of the wildfire, area burned and cause of occurrence. Not all attributes had complete dates – with day, month and year - being some of them indicated with only year of occurrence. For such situations, the attributes were deleted, because the exact day of fire occurrence is critical for the analysis of this study.

The prescribed fire data, in shapefile format, contains both qualitative and easily assessed quantitative elements that describe the burn areas and some behaviour and effects of the fire. For the present study, 70 prescribed fires conducted between the years 2013-2019 (Figure 2) were initially analysed, and their areas ranged from 0.19 ha to 32.3 ha.

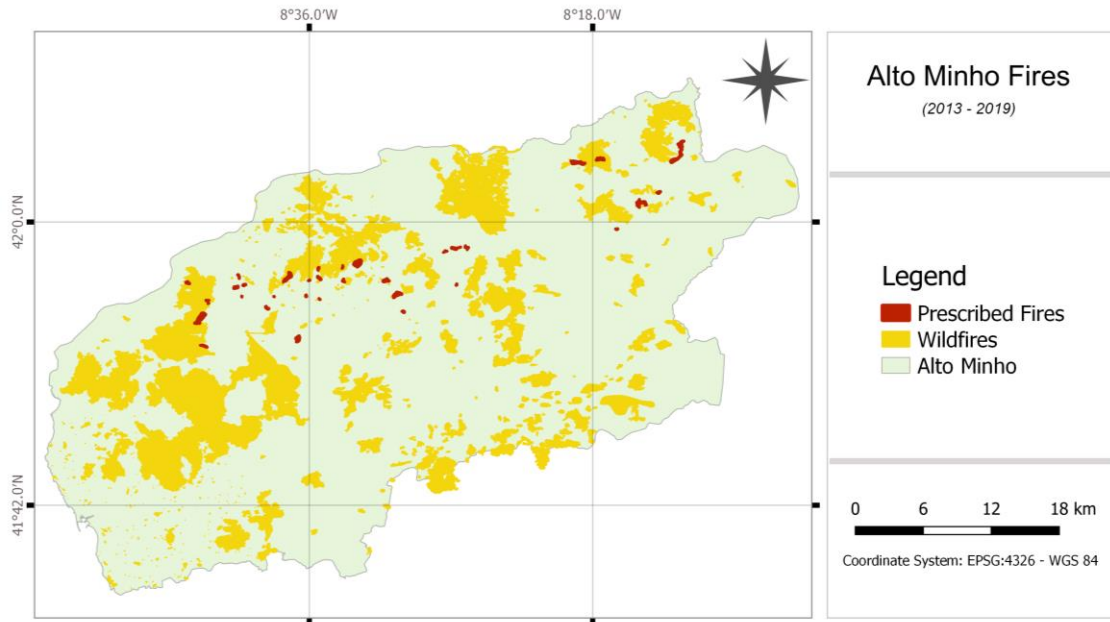


Fig 2. Prescribed fires and wildfires occurrences between 2013 and 2019 in Alto Minho subregion.

Data on land-use for the years 2010 and 2015 (0.5 meters resolution) were retrieved from the Portuguese Geographic Institute (IGP), and together with the prescribed-fire-areas information on slope, aspect, altitude and day of burning, the first dataset was created. These polygons were then used to find similar wildfires to allocate the area of the prescribed fire inside the area of the wildfire, in order to have the same area and shape. Therefore, the wildfires used in this study had the same format and land-use, similar altitude, aspect and slope, and took place in either the same season as the prescribed fire, or in the summer of that same year.

As a result of the allocation of the prescribed fires polygons inside wildfires polygons, two scenarios were created, depending on the day of the wildfire: the wildfires in the summer (when fuel is dry and fire severity is expected to be higher) and wildfires in the winter/autumn, when fire severity is expected to be lower due to the moister weather.

Sampling

In order to minimize border effects, the polygons smaller than one hectare and with a distance from border to border smaller than 60 meters were excluded from the analysis. The 60 meters value was used due to the Landsat resolution of 30 meters. After that, an inner buffer of 30 m was added to the remaining polygons for the Landsat analysis, while for the Sentinel analysis, the inner buffer was of 10 m. Figure 3 shows the difference between the same polygon with and

without inner buffer for NBR, where it is possible to see that the variability decreased for the analysis of 10, 25, 50, 75 and 90 percentiles.



Fig 3. Top: NBR of Landsat data in a polygon without buffer. Bottom: NBR of the same polygon with inner buffer of 30 m.

After creating the inner buffer, the number of pixels for each polygon were checked and polygons with less than twenty pixels were excluded from the analyses, in order to have a more robust statistics, more resistant to outliers. For Sentinel 1 (table 1), all 40 polygons had more than twenty pixels and therefore could be used, while for Landsat data (table 2) 13 polygons could be analysed.

Apart from that, the 5 years' temporal analysis returned about 650 images for Sentinel 1 in the period from 3rd October 2014 to 22 May 2020. For Landsat 8 OLI/TIRS there were 252 images from 11 May 2013 to 6 May 2020, while for Landsat 7 ETM+ there were 54 images to analyse covering the period from 27 January 2010 to 19 May of 2013.

Table 1. Number of pixels for each polygon with Sentinel-1 data

Polygon name	N° of pixels	Polygon name	N° of pixels	Polygon name	N° of pixels
PF16_1	1294	PF18_1	1930	PF18_2	1519
Summer16_1	1294	CloseData18_1	1929	CloseData18_2	1517
PF19_2	175	PF19_5	516	PF19_8	580
CloseData19_2	167	CloseData19_5	518	CloseData19_8	581
Summer19_2	174	Summer19_5	520	PF19_10	126
PF19_3	234	PF19_6	580	CloseData19_10	126
CloseData19_3	223	CloseData19_6	581	PF19_11	1086
Summer19_3	221	Summer19_6	580	CloseData19_11	1090
PF19_15	2434	PF19_13	347	PF19_12	461
Summer19_15	2433	CloseData19_13	351	CloseData19_12	458
PF19_16	84	PF19_17	125	PF19_18	895
Summer19_16	85	Summer19_17	123	Summer19_18	901
PF19_19	271	PF19_20	341		
Summer19_19	272	Summer19_20	338		

Table 2. Number of pixels for each polygon with Landsat data

Polygon name	N° of pixels	Polygon name	N° of pixels	Polygon name	N° of pixels
PF13_1	31	PF13_3	8	PF13_5	6
Summer13_1	30	Summer13_3	10	Summer13_5	4
PF13_4	1	PF13_11	2	CloseData13_5	6
Summer13_4	0	Summer13_11	2	PF13_12	23
PF13_7	21	PF13_6	9	Summer13_12	21
Summer13_7	20	Summer13_6	9	CloseData13_12	24
PF16_1	108	PF18_1	175	PF18_2	123
Summer16_1	108	CloseData18_1	170	CloseData18_2	125
PF19_2	8	PF19_5	11	PF19_8	44
CloseData19_2	8	CloseData19_5	11	CloseData19_8	42
Summer19_2	9	Summer19_5	11	PF19_10	5
PF19_3	9	PF19_6	28	CloseData19_10	6
CloseData19_3	7	CloseData19_6	29	PF19_11	87
Summer19_3	8	Summer19_6	29	CloseData19_11	85
PF19_15	202	PF19_13	23	PF19_12	29
Summer19_15	201	CloseData19_13	23	CloseData19_12	29
PF19_16	1	PF19_17	2	PF19_18	75
Summer19_16	2	Summer19_17	3	Summer19_18	75
PF19_19	15	PF19_20	17		
Summer19_19	13	Summer19_20	19		

Data Analysis

SAR

Google Earth Engine (GEE) provides pre-processed GRD products with σ_0 (sigma-naught) of VV and VH polarizations, after processing for removing thermal noise, calibrating radiometry and converting β_0 beta-naught to sigma-naught using a digital elevation model (DEM). The DEM at the latitudes of the analysed study areas used is from the Shuttle Radar Topography Mission (SRTM) that took place in february 2000 (Farr et al., 2007). Sigma-naught is provided in dB by transformation the backscatter value $Y=10*\log_{10}(X)$ (Small, 2011). The GEE product was further transformed to provide gamma-naught (γ_0) values, thus correcting for the local incidence angle with the SRTM product. This removed the bias between ascending and descending orbits that was evident from plotting the data (Figure 4).

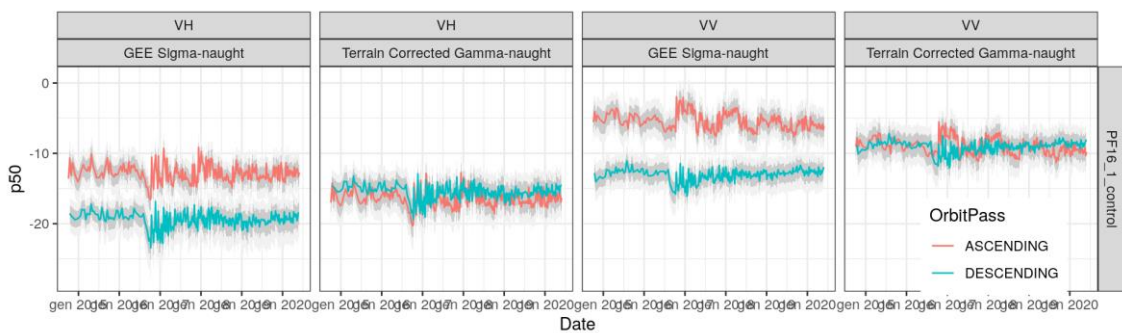


Fig 4. Before and after terrain correction.

The backscatter values can be considered a signal to analyse to detect a significant difference over noise. Noise can be assumed to be the natural variation of backscatter over multiple detections. Over each area, 5 percentiles were extracted using GEE map/reduce methods. It can be noted that it is important to remove outliers; outliers and null values can be from areas falling at the border of an image, even if falling inside the image footprint, such as Figure 5. Falling inside the footprint will include the image/area pair to be used in the map/reduce process, but will produce either null values or very low values that must be removed.

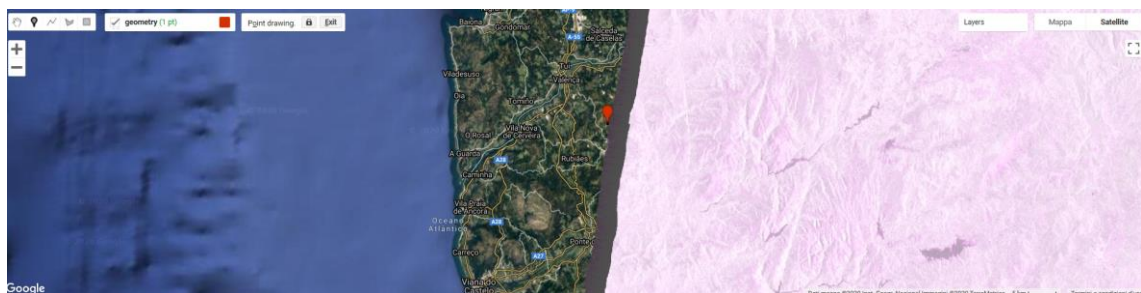


Fig 5. Location of a polygon inside the image footprint

The values extracted by map/reduce were five percentiles $P_n = \{P10, P25, P50, P75, P90\}$. These were available for both VV and VH polarizations. The following combinations were also used:

$$\begin{aligned}
\text{IPr1} &= Y_{p75} - Y_{p25} \\
\text{IPr2} &= Y_{p90} - Y_{p10} \\
\text{NSR}_{pn} &= \frac{Y_{pn}^{VV} - Y_{pn}^{VH}}{Y_{pn}^{VV} + Y_{pn}^{VH}} \quad (1) \\
\text{RATIO}_{pn} &= \frac{Y_{pn}^{VV}}{Y_{pn}^{VH}} \\
\text{DIFF}_{pn} &= Y_{pn}^{VV} - Y_{pn}^{VH}
\end{aligned}$$

Where: P_n is n^{th} percentile and $n = \{10^{\text{th}}, 25^{\text{th}}, 50^{\text{th}}, 75^{\text{th}}, 90^{\text{th}}\}$; NSR is Normalized Signal Ratio; IPr1 and IPr2 are Inter Percentile ranges respectively between the 25th - 75th and the 10th - 90th ranges.

A total of 29 variables were tested and the explanation for each one of them is presented on Table 3.

Table 3. 29 variables used to analyse SAR data

Name of Variables	Explanation
VH_p10; VH_p25; VH_p50; VH_p75; VH_p90	VH polarization over the percentiles taken directly from the Sentinel-1 dataset in GEE
VHRange_p75p25; VHRange_p90p10	Inter-percentile ranges over VH polarization
VV_p10; VV_p25; VV_p50; VV_p75; VV_p90	VV polarization over the five percentiles taken directly from the Sentinel-1 dataset in GEE
VVdivVH_p10; VVdivVH_p25; VVdivVH_p50; VVdivVH_p75; VVdivVH_p90	RATIO over the five percentiles
VVminusVH_p10; VVminusVH_p25; VVminusVH_p50; VVminusVH_p75; VVminusVH_p90	DIFF over the five percentiles
VVnormDiffVH_p10; VVnormDiffVH_p25; VVnormDiffVH_p50; VVnormDiffVH_p75; VVnormDiffVH_p90	NSR over the five percentiles
VVRange_p75p25; VVRange_p90p10	Inter-percentile ranges over VV polarization

To choose which variables gave the best results, this study used a method of rating the variables as “yes” or “no”, based on their capacity of distinguishing a fire event, without giving a false positive response. This method was used in order to select one or even a few best variables that would be compared to the

spectral indices afterwards, since the comparison of all variables with the spectral indices would be an overwhelming analyses.

The Smoothed Z-score algorithm (Brakel, 2016) used to analyse the data aims at detecting backscatter values that significantly change with respect to “normal” values. It can be assumed that, providing a stable surface characteristic over time, backscatter values provide a normally distributed population with a certain average and standard deviation. In the discussion section it is argued that this means the applicability of the method must account for snow and rainfall that change the properties of the surface and thus can provide false positives.

The detection algorithm uses a Z-score calculated using the average (μ) and standard deviation (σ) over a moving window p of size N from values preceding value to be tested. The Z-score of the tested value (Y) is calculated as $Z_x = \frac{Y_x - \mu_p}{\sigma_p}$ where $\mu = \sum_{n=1}^p Y_{n-1}$. If Z is above a certain threshold, then the backscatter value can be considered significantly different from past values. In this work we used a threshold of 3, to achieve a confidence level of 99% or better. This algorithm is used in several applications ranging from detecting acceleration (Esnaola-Gonzalez et al., 2020) to identifying anomalous ribosome footprint (Perkins & Heber, 2018).

Spectral Indices

In this part of the study, the Enhanced Thematic Mapper Plus - ETM+/Landsat 7 was used for collecting data from 2010 and 2013, while the Operational Land Imager - OLI/Landsat 8 images were used from 2013 to 2020. The ETM+ scenes were used only for prescribed fires and wildfires that took place in 2013. That was needed in order to take the average of at least two years prior to the fire event.

The calculated spectral indices were the Normalized Burn Ratio (NBR) (Eq. 2) and the Normalized Difference Vegetation Index (NDVI) (Eq. 3), since they are the most common indices to evaluate fire severity (Escuin et al., 2008; Mallinis et al., 2018)

$$NBR = \frac{NIR - SWIR}{NIR + SWIR} \quad (2)$$

$$NDVI = \frac{NIR - RED}{NIR + RED} \quad (3)$$

Where: NIR - near infrared (ETM+: 4; OLI: 5); SWIR – short wave infrared (ETM+: 7; OLI: 7).

The NDVI and NBR values vary from -1 to 1, being 1 the greater vegetative activity, and values close to zero and negatives indicate little or no chlorophyll activity (Chuvieco et al., 2002).

The spectral indices values of each scene were extracted for 10, 25, 50, 75 and 90 percentiles of pixels of each burned area, then the boxplots representative of the distribution of these values were plotted, following the same methodology used by (dos Santos, Romeiro, de Assis, Torres, & Gleriani, 2018), in order to see the duration of burn scar on the landscape and be able to check if

the treatments (prescribed fires, winter/autumn wildfires and summer wildfires) have the same regeneration time.

After having the plots for Sentinel-1 data and the plots for NDVI and NBR, the comparison between them was made in order to check if SAR gives the right response for a fire event. The summarized work methodology is presented on Figure 6.

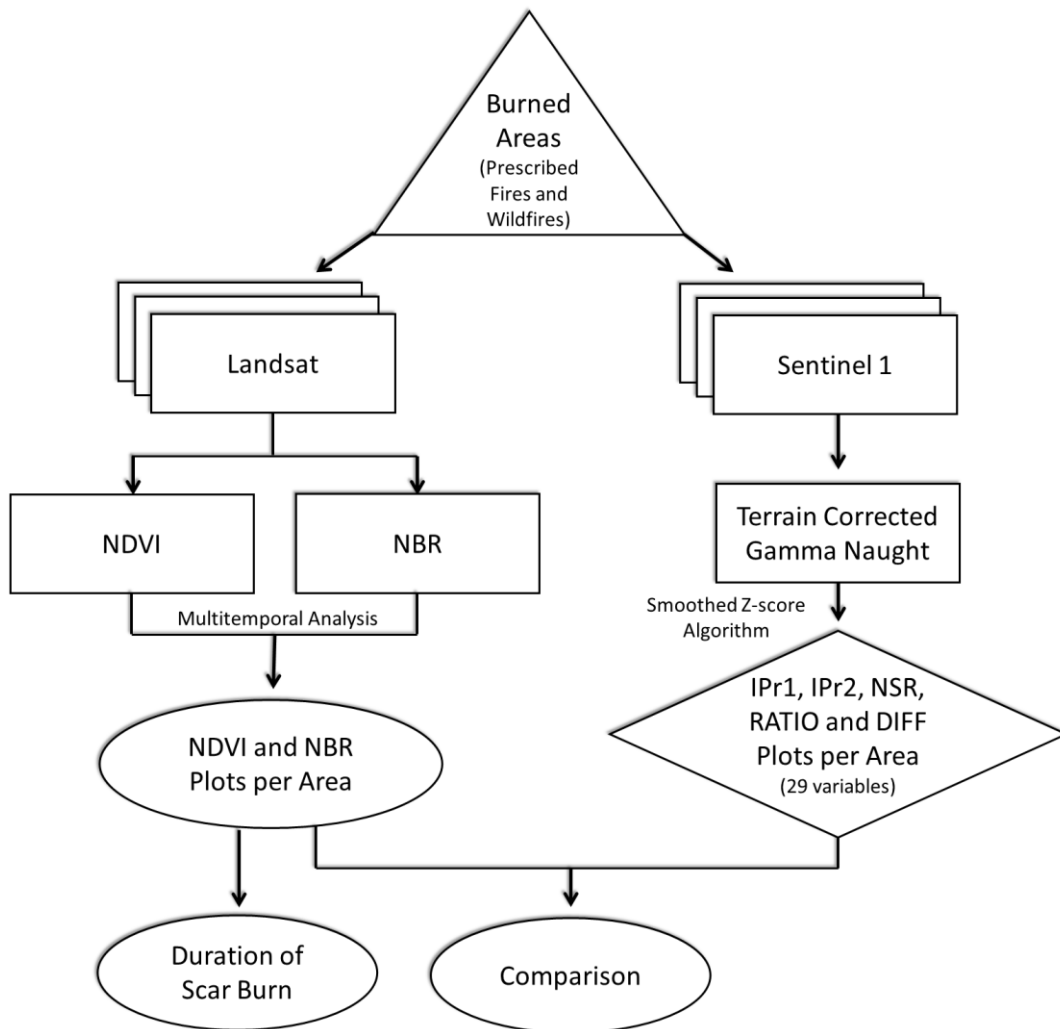


Fig 6. Summarized work methodology

Results

NDVI

On table 4, the “mean before fire” was created using the already stabilized values from all prior data to the fire, meaning that if in the past there was a fire in that same polygon, then this piece of data and its recovery period was not included in the data to create the “mean before fire”. The “minimum after fire” was created using the minimum value of the 50th percentile (i.e. the median), after the fire event, and it takes into account all pixels inside each area. The 50th percentile was chosen due its fewer sensibility to outliers (e.g. unburned parts). The “days for recovery” were calculated based on the 50th percentile value of the first day of fire until the day when the 50th percentile value reaches the “mean before fire”. Finally, the difference between Minimum and Mean (“Min – Mean”) was used to define the severity of the fire in that area.

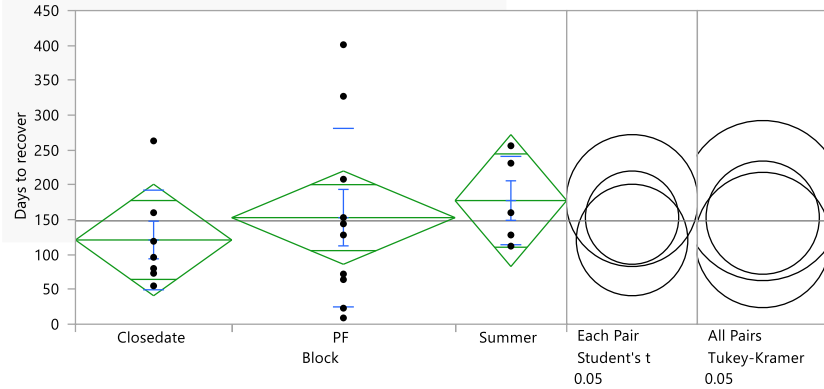
Table 4. Data for each polygon used in NDVI analyses

Block	Polygon	Days for recovery	Day of recovery	Mean Before Fire	SD Before Fire	Minimum After Fire	(Min – Mean)
Winter/Autumn	Winter/Autumn18_1	160	'2-Apr-19'	0.628	0.086	0.260	0.368
Winter/Autumn	Winter/Autumn18_2	263	'14-Jul-19'	0.672	0.054	0.182	0.490
Winter/Autumn	Winter/Autumn19_11	96	'5-Jun-19'	0.724	0.053	0.267	0.457
Winter/Autumn	Winter/Autumn19_12	80	'21-Jun-19'	0.651	0.066	0.353	0.298
Winter/Autumn	Winter/Autumn19_13	73	'5-Jun-19'	0.671	0.080	0.427	0.244
Winter/Autumn	Winter/Autumn19_6	55	'27-May-19'	0.659	0.112	0.410	0.249
Winter/Autumn	Winter/Autumn19_8	119	'28-Jun-19'	0.753	0.056	0.321	0.432
PF	PF13_1	72	'27-Jun-13'	0.610	0.064	0.354	0.256
PF	PF13_12	401	'7-Jun-14'	0.554	0.057	0.339	0.215
PF	PF13_7	64	'27-Jun-13'	0.570	0.073	0.363	0.207
PF	PF16_1	208	'30-May-17'	0.712	0.075	0.335	0.377
PF	PF18_1		N/A	0.681	0.065	0.275	0.406
PF	PF18_2	23	'3-Jan-19'	0.657	0.082	0.470	0.187
PF	PF19_11	327	'5-Dec-19'	0.611	0.056	0.303	0.308
PF	PF19_12	144	'24-Aug-19'	0.705	0.070	0.389	0.316
PF	PF19_13	128	'28-Jun-19'	0.657	0.045	0.393	0.264
PF	PF19_15		N/A	0.698	0.059	0.355	0.343
PF	PF19_18		N/A	0.739	0.041	0.418	0.321
PF	PF19_6	9	'1-Mar-19'	0.683	0.052	0.603	0.080
PF	PF19_8	153	'5-Jun-19'	0.574	0.061	0.384	0.190
Summer	Summer13_1	231	'13-May-14'	0.539	0.085	0.140	0.399
Summer	Summer13_12	256	'13-May-14'	0.588	0.085	0.239	0.349
Summer	Summer13_7	128	'29-Dec-13'	0.613	0.068	0.168	0.445
Summer	Summer16_1	112	'5-Dec-16'	0.674	0.072	0.279	0.395
Summer	Summer19_15		N/A	0.741	0.045	0.236	0.505
Summer	Summer19_18	160	'10-Mar-20'	0.659	0.096	0.294	0.365
Summer	Summer19_6		N/A	0.649	0.065	0.250	0.399

Where: PF means Prescribed Fires; N/A means the polygon has not recovered from the fire until the last day of analysis (26/03/2020).

As reported in Figure 8, for the duration of burn scar, the wildfires that took place during winter/autumn took an average of 121 days to recover from the fire, while the wildfires that happen in summer took an average of 177 days and the prescribed fires had an average of 152 days to recover. The number of days to recover from the fire for all three treatments (winter/autumn wildfires, summer wildfires and prescribed fires) were considered equal by the Tukey test ($p < 0.05$). The box-plots for each area are presented in Appendix 3.

Oneway Analysis of Days for vegetation recovery By Block



Analysis of Variance

Source	DF	Sum of Squares	Mean Square	F Ratio	Prob > F
Block	2	9717	4859	0.475	0.629
Error	19	194355	10229		
C. Total	21	204072			

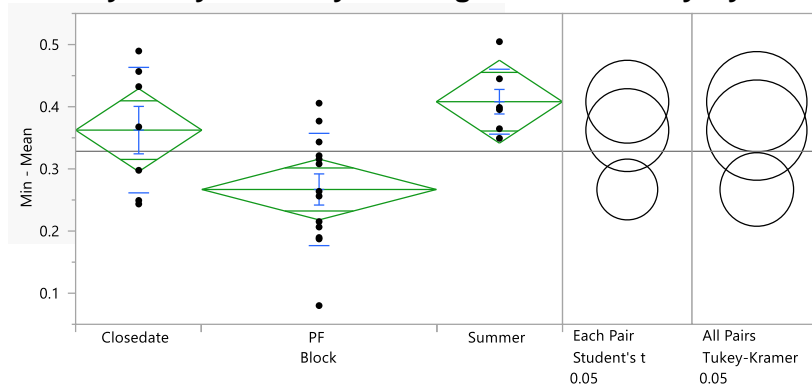
Comparisons for all pairs using Tukey-Kramer HSD

Level	Mean
Summer	A 177
PF	A 153
Winter/Autumn	A 121

Fig 8. Summary of the statistical analysis for numbers of days to recover from fire using NDVI

As discussed before, NDVI and NBR are often used to assess the severity of wildfires, and the greater the difference (pre- and post-fire), the greater the severity. As shown in Figure 9, for the difference between pre-fire and post-fire responses of NDVI, the winter/autumn wildfires, the summer wildfires and the prescribed fires had an average pre- and post-fire difference of 0.362, 0.408 and 0.266, respectively. The winter/autumn wildfires are considered, by the Tukey test, as not having significantly different severity from the prescribed fires. On the other hand, severity of summer wildfires differs significantly from severity of prescribed fires, while also being similar to winter/autumn wildfires.

Oneway Analysis of Days for vegetation recovery By Block



Analysis of Variance

Source	DF	Sum of Squares	Mean Square	F Ratio	Prob > F
Block	2	0.102	0.051	6.961	0.0041*
Error	24	0.175	0.007		
C. Total	26	0.277			

Comparisons for all pairs using Tukey-Kramer HSD

Level	Mean
Summer	A 0.408
Winter/Autumn	A B 0.362
PF	B 0.267

Fig 9. Summary of the statistical analysis for severity of fire, using NDVI.

NBR

On table 5, all the variables were created using the previously explained methodology, but this time taking into account the NBR values.

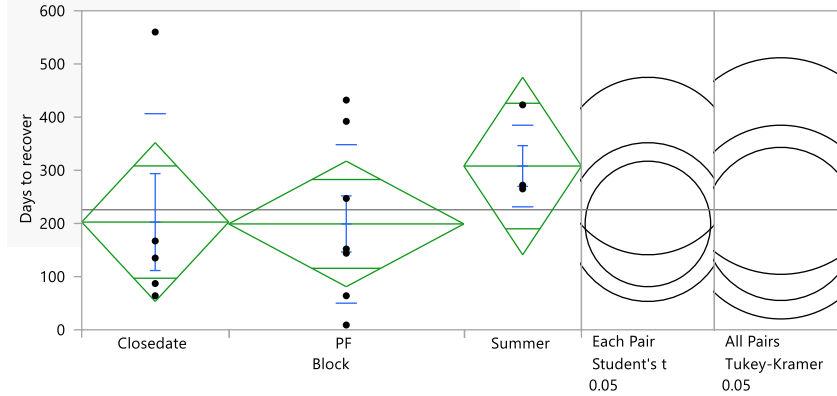
Table 5. Data for each polygon used in NBR analyses

Block	Polygon	Days for recovery	Day of recovery	Mean Before Fire	SD Before Fire	Minimum After Fire	(Min - Mean)
Winter/Autumn	Winter/Autumn18_1	167	'9-Apr-19'	0.374	0.156	-0.178	0.552
Winter/Autumn	Winter/Autumn18_2	560	'6-May-20'	0.486	0.068	-0.381	0.867
Winter/Autumn	Winter/Autumn19_11	135	'14-Jul-19'	0.520	0.082	-0.28	0.800
Winter/Autumn	Winter/Autumn19_12		N/A	0.425	0.082	-0.299	0.724
Winter/Autumn	Winter/Autumn19_13	64	'27-May-19'	0.439	0.140	0.019	0.420
Winter/Autumn	Winter/Autumn19_6	87	'28-Jun-19'	0.508	0.098	-0.143	0.651
Winter/Autumn	Winter/Autumn19_8		N/A	0.581	0.061	-0.322	0.903
PF	PF13_1	392	'13-May-14'	0.437	0.083	-0.158	0.595
PF	PF13_12	152	'1-Oct-13'	0.336	0.127	-0.205	0.541
PF	PF13_7	64	'27-Jun-13'	0.350	0.154	-0.125	0.475
PF	PF16_1	247	'8-Jul-17'	0.534	0.079	-0.225	0.759
PF	PF18_1		N/A	0.494	0.066	-0.167	0.661
PF	PF18_2		N/A	0.511	0.061	0.185	0.326
PF	PF19_11	432	'19-Mar-20'	0.390	0.071	-0.206	0.596
PF	PF19_12		N/A	0.518	0.075	-0.196	0.714
PF	PF19_13	144	'14-Jul-19'	0.435	0.063	-0.027	0.462
PF	PF19_15		N/A	0.513	0.068	-0.075	0.588
PF	PF19_18		N/A	0.582	0.051	0.053	0.529
PF	PF19_6	9	'1-Mar-19'	0.517	0.074	0.417	0.100
PF	PF19_8	153	'5-Jun-19'	0.302	0.086	-0.097	0.399
Summer	Summer13_1	272	'7-Jun-14'	0.382	0.079	-0.294	0.676
Summer	Summer13_12	265	'22-May-14'	0.341	0.147	-0.432	0.773
Summer	Summer13_7	423	'20-Oct-14'	0.482	0.083	-0.433	0.915
Summer	Summer16_1	272	'14-May-17'	0.484	0.078	-0.123	0.607
Summer	Summer19_15		N/A	0.565	0.062	-0.202	0.767
Summer	Summer19_18		N/A	0.416	0.165	-0.307	0.723
Summer	Summer19_6		N/A	0.429	0.091	-0.365	0.794

Where: PF means Prescribed Fires; N/A means the polygon has not recovered from the fire until the last day of analysis (26/03/2020).

As reported in Figure 10, for the duration of burn scar by NBR, the winter/autumn wildfires had an average of 202 days to recover from the fire, while the summer wildfires had an average of 308 days and the prescribed fires had an average of 199 days to recover from the burning. The number of days to recover from the fire for all three treatments were considered equal by the Tukey test ($p < 0.05$).

Oneway Analysis of Days for vegetation recovery By Block



Analysis of Variance

Source	DF	Sum of Squares	Mean Square	F Ratio	Prob > F
Block	2	35411	17706	0.731	0.499
Error	14	339328	24238		
C. Total	16	374739			

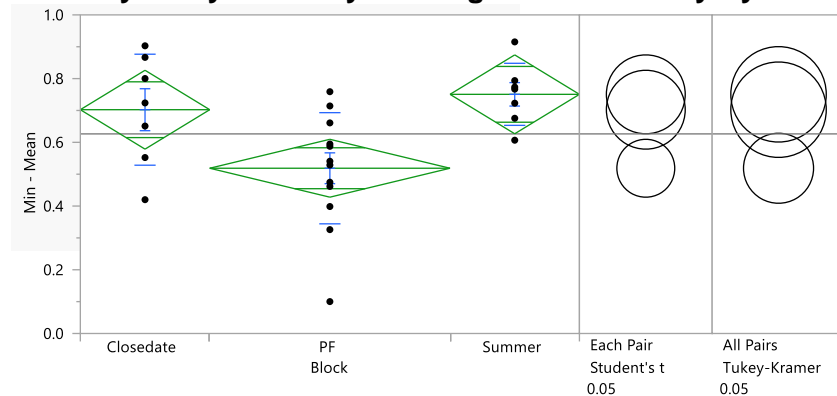
Comparisons for all pairs using Tukey-Kramer HSD

Level		Mean
Summer	A	308
Winter/Autumn	A	203
PF	A	199

Fig 10. Summary of the statistical analysis for numbers of days to recover from fire using NBR

For Figure 11, the difference between pre-fire and post-fire responses for winter/autumn wildfires, summer wildfires and prescribed fires had an average of 0.702, 0.751 and 0.519, respectively. The winter/autumn wildfires are considered by the Tukey test of similar severity when compared to the prescribed fires. On the other hand, severity of summer wildfires is significantly different from severity of prescribed fires, while also being similar to winter/autumn wildfires. Specially, the areas with the lower fire severity were Prescribed Fire 2019_8 (PF19_8), Prescribed Fire 2019_6 (PF 19_6) and Prescribed Fire 2018_2 (PF 18_2).

Oneway Analysis of Days for vegetation recovery By Block



Analysis of Variance

Source	DF	Sum of Squares	Mean Square	F Ratio	Prob > F
Block	2	0.299	0.150	5.945	0.0080*
Error	24	0.604	0.025		
C. Total	26	0.904			

Comparisons for all pairs using Tukey-Kramer HSD

Level		Mean
Summer	A	0.751
Winter/Autumn	A B	0.702
PF	B	0.519

Fig 11. Summary of the statistical analysis for fire severity, using NBR.

SAR

The images in Appendix 1 show an example from one area over the 29 different variables - green line is the averaged line over past 30 values, the black line is the values and the grey area is the standard deviation. The red points are all signals considered as significantly different from past signal. This was defined using the Z-score of each value calculated using the mean and standard deviation of the past 30 values; a Z-score above 3 was defined as significantly different.

For the 29 variables, when analysed by visual interpretation without comparing them with spectral indices, the variable that gave the best results ($p = 0.0028$) was VVnormDiffVH_p90 (NSR percentile 90), being able to detect fire events 19 times out of the 39 areas (48% of correct responses) – without false positive and false negative responses. VVnormDiffVH_p75, VV_p50, VV_p90, VV_p75, VV_p25, VV_p90, VH_p50, VVdivVH_p75 and VVdivVH_p90 were also considered as good ($p < 0.0001$), with an average of 14.6 times as correct responses to fire. The variables with the most ($p < 0.0001$) wrong responses to fires were VHRange_p75p25, VHRange_p90p10, VVRange_p75p25, VVRange_p90p10, with an average of only 3.25 times of right responses to fires.

SAR and spectral indices comparison

For this part of the study, only the NSR percentile 90 was used, in an attempt to make the comparison easier. Also, only areas with NDVI and NBR data and SAR data were used (20 in total). That was needed because Sentinel-1 A was only launched in 2014, therefore all areas that burned in 2013 could not be analysed by SAR.

The NBR and NDVI plots were adapted to look more similar to the SAR plots and to also make the visual interpretation more direct. For that reason, the plots now are presented with the mean value before fire and its standard deviation in green. The grey region is the percentile 10 and 90 for the black line represents the percentile 50. The red line indicates the fire event that was the focus of comparison and the red dotted line, that is shown in some plots, indicates a fire that was identified by the spectral indices and confirmed by the official data from the Institute for Nature Conservation and Forests (ICFN).

In some cases, it is possible to see that even though the spectral indices behave like there was a fire occurrence (e.g. Summer Wildfire 2019_18, Winter Wildfire 2018_1), there is no indication of a fire – with the red dotted line – because according to the official data from ICFN, there was no fire on that day.

In Figure 12 there is a sample of two comparisons where Sentinel-1 worked properly, another one where SAR responded wrongly and a third one where it is possible to observe that the spectral indices dropped to negative values where in theory a fire would not have happened, and SAR had the same behaviour in this case.

The full set of plots are presented in Appendix 2 and when both NSR percentile 90 and the spectral indices are compared, the rating of correct responses for SAR improve considerably, since SAR responded accordingly to NBR 19 out of 20 times (95% of correct responses) – being the “Prescribed Fire 19_6” the only one that substantially differed from NBR and NDVI values, and also one of the areas with lower fire severity.

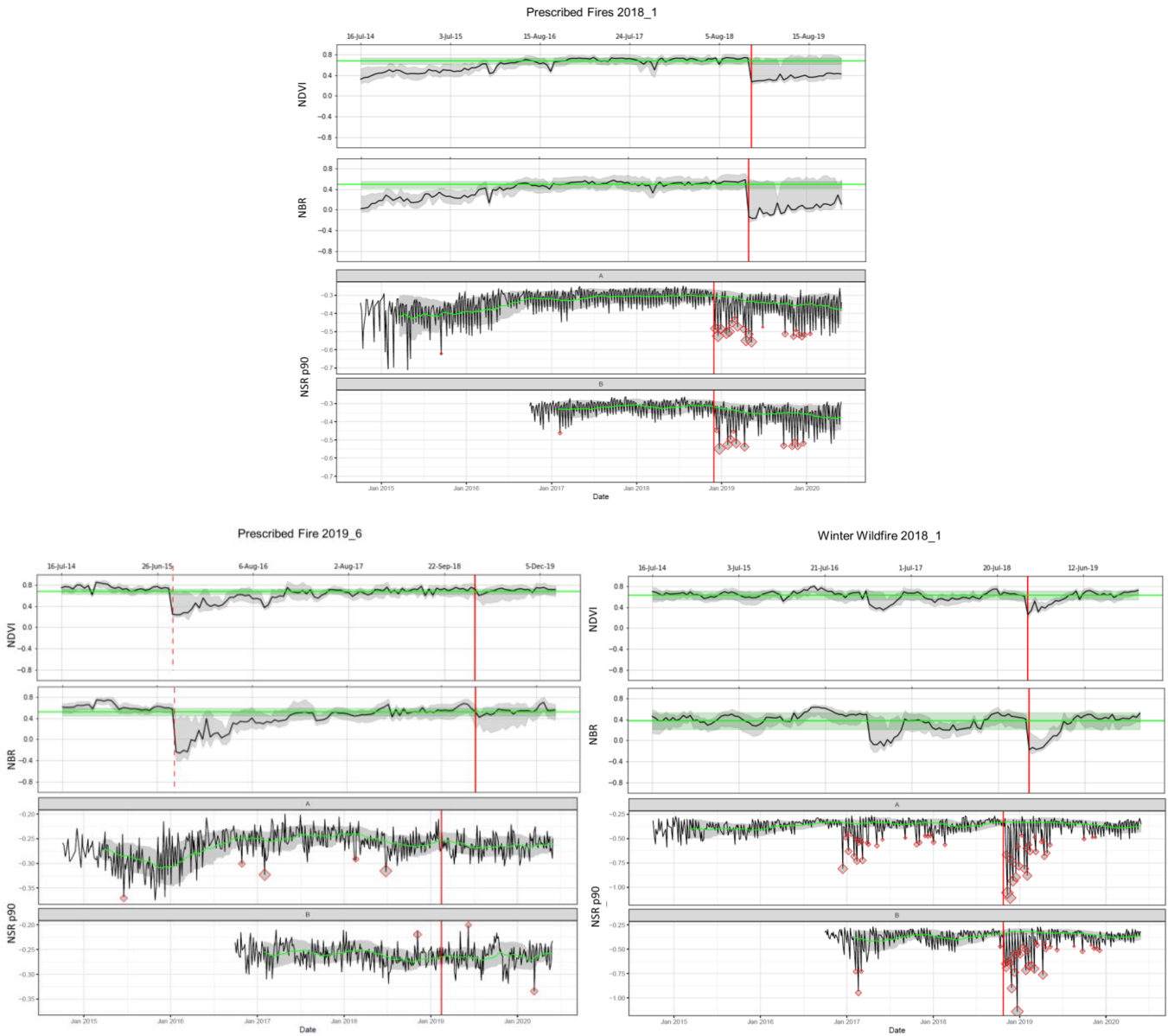


Figure 12. SAR and spectral indices comparison. Upper image is an example of SAR NSR percentile 90 working perfectly in accordance to the fire event. Bottom right image is where SAR and the spectral indices dropped their values. Bottom left image shows SAR identifying fires inappropriately.

Discussion

For the assessment on how Sentinel-1 works for wildfires and prescribed fires, the variable NSR p_90 (VVnormDiffVH_p90) was considered as the best one from the 29 analysed, and in contradiction to Imperatore et al., (2017), the VH polarization alone did not effectively respond to the fire occurrences. Furthermore, even though the variable NSR p_90 was considered as correctly responding to fire events only 48% of the times, the method used was strict to the corresponding answers to fires indicated on the official data from ICFN and did not tolerate false positive answers, like would be the case if one value dropped without any indication of fires on the official data from ICFN. Therefore, 48% of the times when NSR p_90 showed a fire event and an absence of fires, the fire/absence of fire was confirmed on the official data.

Although this was the method used to evaluate what variable would be the best one between all the 29, once the chosen variable (NSR p_90) was confronted with NBR/NDVI, the percentage of correct responses increased significantly. That is because even NBR and NDVI gave theoretically false positive answers for most of the areas that were considered as wrong fire detection for NSR p_90. When both NSR percentile 90 and the spectral indices were compared, the rating of correct responses for SAR improved considerably, since SAR responded accordingly to NBR 95% of the times. That means that, if NBR is the most used index for its right responses to fire, NSR percentile 90 could be considered as a good fit as well.

Moreover, in some cases it is possible to see that even though the spectral indices behave like there was a fire occurrence (e.g. NBR 19_18 Summer), there is no indication of a fire in the official data from ICFN. This issue might mirror another case (dos Santos et al., 2018) where official reports do not match the spectral indices responses, and to investigate this issue, a future study would have to be conducted.

It is also important to note that the present research only took into consideration burned areas covered by grasses and small bushes, therefore future studies should focus on using SAR and comparing its values to spectral indices values in different land-uses.

For the evaluation if wildfires have similar fire severity when compared to prescribed fires, even though the number of days to recover from the fire for all three treatments (winter/autumn wildfires, summer wildfires and prescribed fires) were considered as equal, the winter/autumn wildfires are considered of similar severity when compared to the prescribed fires. On the other hand, severity of summer wildfires is significantly different from severity of prescribed fires, while also being similar to winter/autumn wildfires. Therefore, it can be argued that in this scenario the summer wildfires have a stronger impact on the surface, but this does not affect the time it takes to recover.

The fact that winter/autumn wildfires have similar severity to the prescribed fires could be used as an advantage to the forest managers, since the lack of resources make it impossible to treat the necessary area of the landscape every year, making prescribed burnings almost ineffective on wildfire extent (P. M. Fernandes, 2015). Therefore, for the sake of management, winter wildfires could be used as a treatment to reduce summer wildfires, but it is extremely important to take into account that there is no previous delimitation for any wildfire and the risk for people and infrastructure still needs to be taken into account, even if the wildfire is of low severity.

Conclusions

The findings of the study raise some managerial implications two of which are worth to be addressed here.

One, NSR percentile 90 seems to work properly for areas of grasses and small bushes when assessing burn areas, but it also seems to work best when the fire severity in the area is greater.

It is worth noting that, the NSR percentile 90 was initially considered as correctly responding to fire events only 48% of the times where the official fire data from ICFN was used as support, but after comparing the SAR values to NBR values, the percentage of “right” responses increased significantly – to 95%. That could be either due to a real difference between NBR and the official fire data from ICFN, or it could be due to bias. To investigate this issue diminishing the human bias, the comparison between NSR p_90 and NBR could be automatized in future studies.

Two, winter/autumn wildfires have a severity close to the severity that prescribed fires have, therefore they could be used a treatment to reduce summer wildfires, but with caution since there are real risks related to wildfires for people and infrastructure. What can be concluded from this finding is that Meteorological conditions are the responsible for defining severity of fires, since all other variables (altitude, slope, aspect, area, shape and land-use) were equal or similar for all areas analysed.

Therefore, as a managerial implication, if the weather conditions at the time of the wildfire occurrence are normal for the season (winter/autumn), and firefighters have analysed the situation, established a perimeter in the area that is safe to burn and unsure that safety conditions are settled, then the occurrence can be monitored without giving direct combat over the fire. In this case, combating the fire is only needed if the fire exceeds the perimeter.

Bibliography

- Airey Lauvaux, C., Skinner, C. N., & Taylor, A. H. (2016). High severity fire and mixed conifer forest-chaparral dynamics in the southern Cascade Range, USA. *Forest Ecology and Management*, 363, 74–85.
<https://doi.org/10.1016/j.foreco.2015.12.016>
- Alexander, J. D., Seavy, N. E., Ralph, C. J., & Hogoboom, B. (2006). Vegetation and topographical correlates of fire severity from two fires in the Klamath-Siskiyou region of Oregon and California. *International Journal of Wildland Fire*, 15(2), 237–245. <https://doi.org/10.1071/WF05053>
- Arkle, R. S., Pilliod, D. S., & Welty, J. L. (2012). Pattern and process of prescribed fires influence effectiveness at reducing wildfire severity in dry coniferous forests. *Forest Ecology and Management*. <https://doi.org/10.1016/j.foreco.2012.04.002>
- Chen, X., Vogelmann, J. E., Rollins, M., Ohlen, D., Key, C. H., Yang, L., ... Shi, H. (2011). Detecting post-fire burn severity and vegetation recovery using multitemporal remote sensing spectral indices and field-collected composite burn index data in a ponderosa pine forest. *International Journal of Remote Sensing*, 32(23), 7905–7927. <https://doi.org/10.1080/01431161.2010.524678>
- Chuvienco, E., Martín, M. P., & Palacios, A. (2002). Assessment of different spectral indices in the red-near-infrared spectral domain for burned land discrimination. *International Journal of Remote Sensing*.
<https://doi.org/10.1080/01431160210153129>
- Collins, L., Griffioen, P., Newell, G., & Mellor, A. (2018). The utility of Random Forests for wildfire severity mapping. *Remote Sensing of Environment*, 216(December 2017), 374–384. <https://doi.org/10.1016/j.rse.2018.07.005>
- Colson, D., Petropoulos, G. P., & Ferentinos, K. P. (2018). Exploring the Potential of Sentinels-1 & 2 of the Copernicus Mission in Support of Rapid and Cost-effective Wildfire Assessment. *International Journal of Applied Earth Observation and Geoinformation*, 73(June), 262–276. <https://doi.org/10.1016/j.jag.2018.06.011>
- Coppoletta, M., Merriam, K. E., & Collins, B. M. (2015). Post-fire vegetation and fuel development influences fire severity patterns in reburns. *Ecological Applications*, 26(3), 686–699. <https://doi.org/10.1890/15-0225.1>
- Cruz, M. G., Alexander, M. E., & Dam, J. E. (2014). *Characteristics to Evaluate Fuel Treatment*. 60(October), 1000–1004. <https://doi.org/10.5849/forsci.13-719>
- Dillon, G. K., Holden, Z. A., Morgan, P., Crimmins, M. A., Heyerdahl, E. K., & Luce, C. H. (2011). Both topography and climate affected forest and woodland burn severity in two regions of the western US, 1984 to 2006. *Ecosphere*, 2(12), art130.

- <https://doi.org/10.1890/es11-00271.1>
- dos Santos, J. F. C., Romeiro, J. M. N., de Assis, J. B., Torres, F. T. P., & Gleriani, J. M. (2018). Potentials and limitations of remote fire monitoring in protected areas. *Science of the Total Environment*, 616–617, 1347–1355.
<https://doi.org/10.1016/j.scitotenv.2017.10.182>
- Drusch, M., Del Bello, U., Carlier, S., Colin, O., Fernandez, V., Gascon, F., ... Bargellini, P. (2012). Sentinel-2: ESA's Optical High-Resolution Mission for GMES Operational Services. *Remote Sensing of Environment*.
<https://doi.org/10.1016/j.rse.2011.11.026>
- Escuin, S., Navarro, R., & Fernández, P. (2008). Fire severity assessment by using NBR (Normalized Burn Ratio) and NDVI (Normalized Difference Vegetation Index) derived from LANDSAT TM/ETM images. *International Journal of Remote Sensing*, 29(4), 1053–1073. <https://doi.org/10.1080/01431160701281072>
- Eснаоla-Gonzalez, I., Gómez-Omella, M., Ferreiro, S., Fernandez, I., Lázaro, I., & García, E. (2020). An IoT platform towards the enhancement of poultry production chains. *Sensors (Switzerland)*, 20(6), 1–20. <https://doi.org/10.3390/s20061549>
- Farr, T. G., Rosen, P. A., Caro, E., Crippen, R., Duren, R., Hensley, S., ... Alsdorf, D. E. (2007). The shuttle radar topography mission. *Reviews of Geophysics*.
<https://doi.org/10.1029/2005RG000183>
- Fernandes, P., & Botelho, H. (2004). Analysis of the prescribed burning practice in the pine forest of northwestern Portugal. *Journal of Environmental Management*.
<https://doi.org/10.1016/j.jenvman.2003.10.001>
- Fernandes, P. M. (2015). Empirical support for the use of prescribed burning as a fuel treatment. *Current Forestry Reports*, 1(2), 118–127.
<https://doi.org/10.1007/s40725-015-0010-z>
- Fernandes, P. M., & Loureiro, C. (2013). Fine fuels consumption and CO2 emissions from surface fire experiments in maritime pine stands in northern Portugal. *Forest Ecology and Management*, 291, 344–356.
<https://doi.org/10.1016/j.foreco.2012.11.037>
- Finney, M. A., McHugh, C. W., & Grenfell, I. C. (2005). Stand- and landscape-level effects of prescribed burning on two Arizona wildfires. *Canadian Journal of Forest Research*, 35(7), 1714–1722. <https://doi.org/10.1139/x05-090>
- Fulé, P. Z., Crouse, J. E., Roccaforte, J. P., & Kalies, E. L. (2012). Do thinning and/or burning treatments in western USA ponderosa or Jeffrey pine-dominated forests help restore natural fire behavior? *Forest Ecology and Management*, 269, 68–81.
<https://doi.org/10.1016/j.foreco.2011.12.025>
- Gorelick, N., Hancher, M., Dixon, M., Ilyushchenko, S., Thau, D., & Moore, R. (2017).

- Google Earth Engine: Planetary-scale geospatial analysis for everyone. *Remote Sensing of Environment*. <https://doi.org/10.1016/j.rse.2017.06.031>
- Harris, L., & Taylor, A. H. (2017). Previous burns and topography limit and reinforce fire severity in a large wildfire. *Ecosphere*, *8*(11). <https://doi.org/10.1002/ecs2.2019>
- Harvey, B. J., Donato, D. C., & Turner, M. G. (2016). Burn me twice, shame on who? Interactions between successive forest fires across a temperate mountain region. *Ecology*, *97*(9), 2272–2282. <https://doi.org/10.1002/ecy.1439>
- Imperatore, P., Azar, R., Calo, F., Stroppiana, D., Brivio, P. A., Lanari, R., & Pepe, A. (2017). Effect of the Vegetation Fire on Backscattering: An Investigation Based on Sentinel-1 Observations. *IEEE Journal of Selected Topics in Applied Earth Observations and Remote Sensing*, *10*(10), 4478–4492. <https://doi.org/10.1109/JSTARS.2017.2717039>
- Lourenço L, Félix F. The forest fire surge of 2017 in mainland Portugal, the beginning of a fourth “generation” Territorium 2019;26:35-48. doi:10.14195/1647-7723_26-2_3.
- Keeley, J. E. (2009). Fire intensity, fire severity and burn severity: A brief review and suggested usage. *International Journal of Wildland Fire*, *18*(1), 116–126. <https://doi.org/10.1071/WF07049>
- Lentile, L. B., Smith, F. W., & Shepperd, W. D. (2006). Influence of topography and forest structure on patterns of mixed severity fire in ponderosa pine forests of the South Dakota Black Hills, USA. *International Journal of Wildland Fire*, *15*(4), 557–566. <https://doi.org/10.1071/WF05096>
- Mallinis, G., Mitsopoulos, I., & Chrysafi, I. (2018). Evaluating and comparing sentinel 2A and landsat-8 operational land imager (OLI) spectral indices for estimating fire severity in a mediterranean pine ecosystem of Greece. *GIScience and Remote Sensing*, *55*(1), 1–18. <https://doi.org/10.1080/15481603.2017.1354803>
- Oliveira, S., Félix, F., Nunes, A., Lourenço, L., Laneve, G., & Sebastián-López, A. (2018). Mapping wildfire vulnerability in Mediterranean Europe. Testing a stepwise approach for operational purposes. *Journal of Environmental Management*. <https://doi.org/10.1016/j.jenvman.2017.10.003>
- Pereira, J. M. C. (1999). A comparative evaluation of NOAA/AVHRR vegetation indexes for burned surface detection and mapping. *IEEE Transactions on Geoscience and Remote Sensing*, *37*(1 PART 1), 217–226. <https://doi.org/10.1109/36.739156>
- Perkins, P., & Heber, S. (2018). Identification of Ribosome Pause Sites Using a Z-Score Based Peak Detection Algorithm. *IEEE International Conference on Computational Advances in Bio and Medical Sciences, ICCABS, 2018-Octob*, 4–9.

- <https://doi.org/10.1109/ICCABS.2018.8541902>
- Piñol, J., Beven, K., & Viegas, D. X. (2005). Modelling the effect of fire-exclusion and prescribed fire on wildfire size in Mediterranean ecosystems. *Ecological Modelling*, 183(4), 397–409. <https://doi.org/10.1016/j.ecolmodel.2004.09.001>
- Prichard, S. J., Peterson, D. L., & Jacobson, K. (2010). Fuel treatments reduce the severity of wildfire effects in dry mixed conifer forest, Washington, USA. *Canadian Journal of Forest Research*. <https://doi.org/10.1139/X10-109>
- Reinhardt, E. D., Keane, R. E., Calkin, D. E., & Cohen, J. D. (2008). Objectives and considerations for wildland fuel treatment in forested ecosystems of the interior western United States. *Forest Ecology and Management*, 256(12), 1997–2006. <https://doi.org/10.1016/j.foreco.2008.09.016>
- Small, D. (2011). Flattening gamma: Radiometric terrain correction for SAR imagery. *IEEE Transactions on Geoscience and Remote Sensing*, 49(8), 3081–3093. <https://doi.org/10.1109/TGRS.2011.2120616>
- Stroppiana, D., Azar, R., Calò, F., Pepe, A., Imperatore, P., Boschetti, M., ... Lanari, R. (2015). Integration of Optical and SAR Data for Burned Area Mapping in Mediterranean Regions. *Remote Sensing*, 7(2), 1320–1345. <https://doi.org/10.3390/rs70201320>
- Torres, R., Snoeij, P., Geudtner, D., Bibby, D., Davidson, M., Attema, E., ... Rostan, F. (2012). GMES Sentinel-1 mission. *Remote Sensing of Environment*. <https://doi.org/10.1016/j.rse.2011.05.028>
- Veraverbeke, S., Gitas, I., Katagis, T., Polychronaki, A., Somers, B., & Goossens, R. (2012). Assessing post-fire vegetation recovery using red-near infrared vegetation indices: Accounting for background and vegetation variability. *ISPRS Journal of Photogrammetry and Remote Sensing*, 68(1), 28–39. <https://doi.org/10.1016/j.isprsjprs.2011.12.007>
- Wimberly, M. C., Cochrane, M. A., Baer, A. D., & Kari, P. (2009). Assessing fuel treatment effectiveness using satellite imagery and spatial statistics. *Ecological Applications*. <https://doi.org/10.1890/08-1685.1>

Websites

Brakel, J. Smoothed Z-Score Algorithm, 2016. Available online: <http://stackoverflow.com/questions/22583391/peak-signal-detection-in-realtime-timeseries-data> (accessed on 10 June 2020).

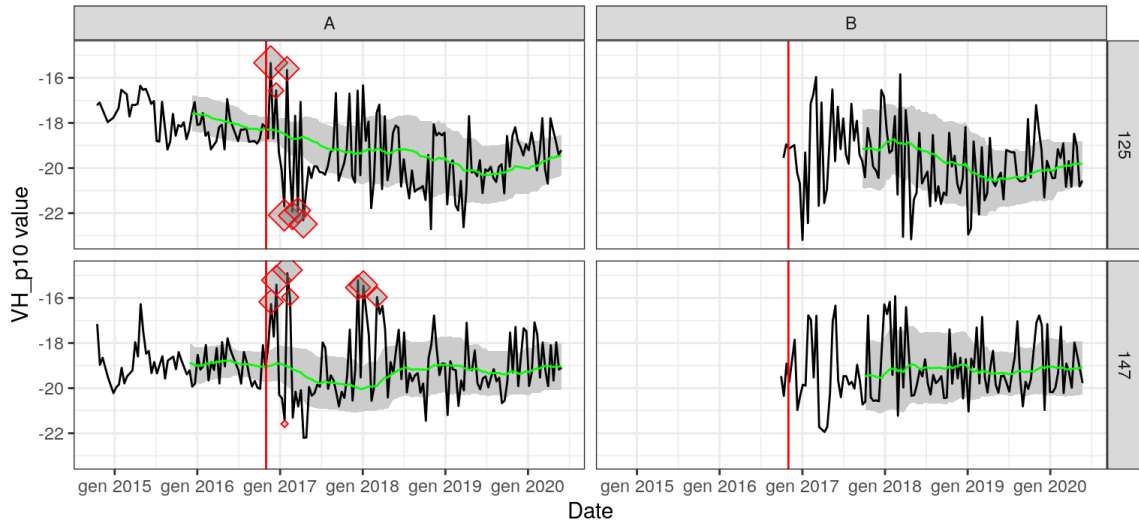
ICNF - Instituto da Conservação da Natureza e das Florestas. URL.<https://www.icnf.pt/>, Accessed date: 30 May 2020.

IPMA - Instituto Português do Mar e da Atmosfera. Normais Climatológicas. URL. <http://www.ipma.pt/pt/oclima/normais.clima/>, Accessed date: 30 May 2020.

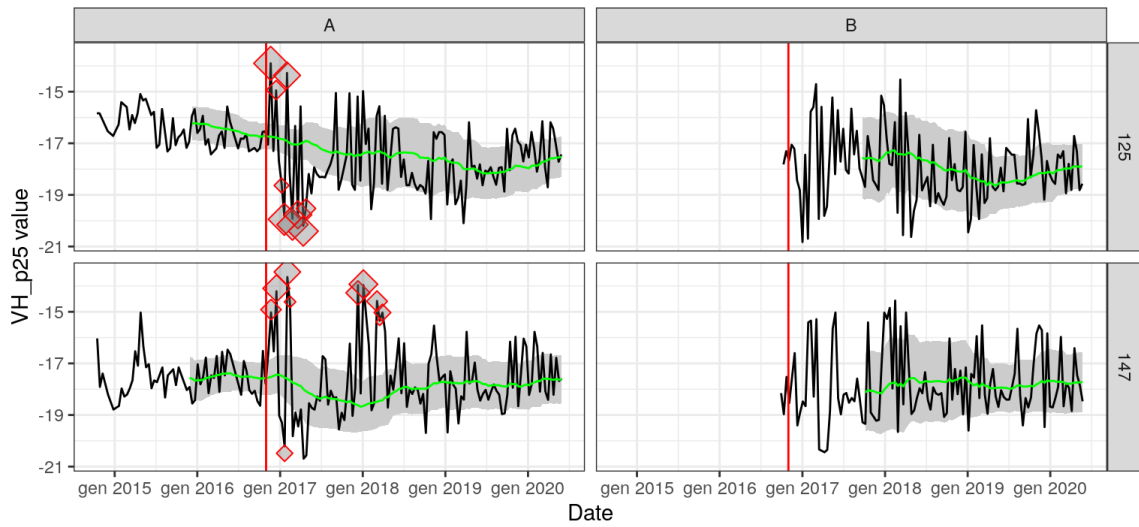
Appendix

Appendix 1 – Values of the 29 SAR indices on one area. Column A and B represent Sentinel-1A and 1B respectively. Rows represent the orbit number.

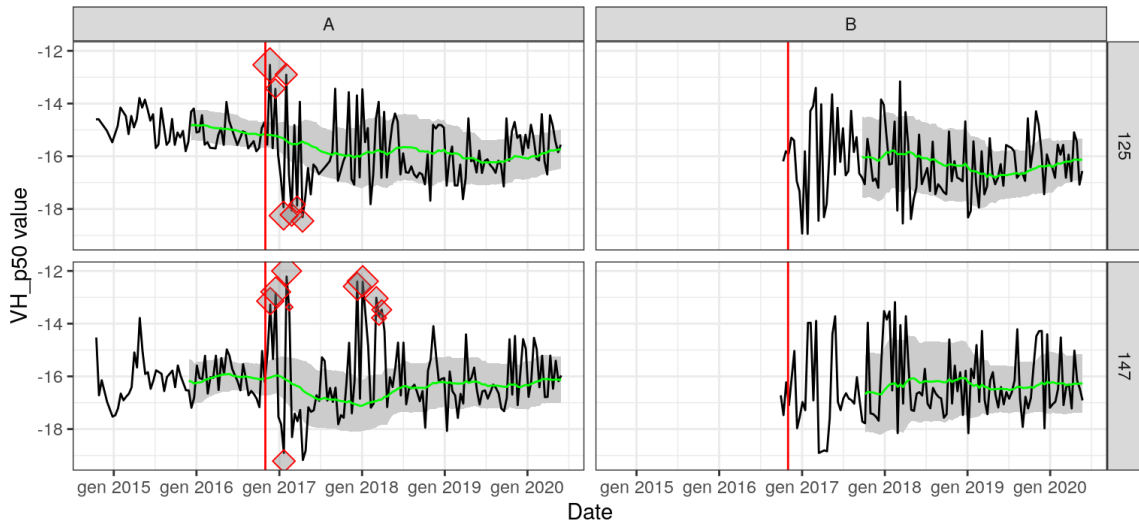
Area: PF16_1 - Variable: VH_p10 - Z-score > 3



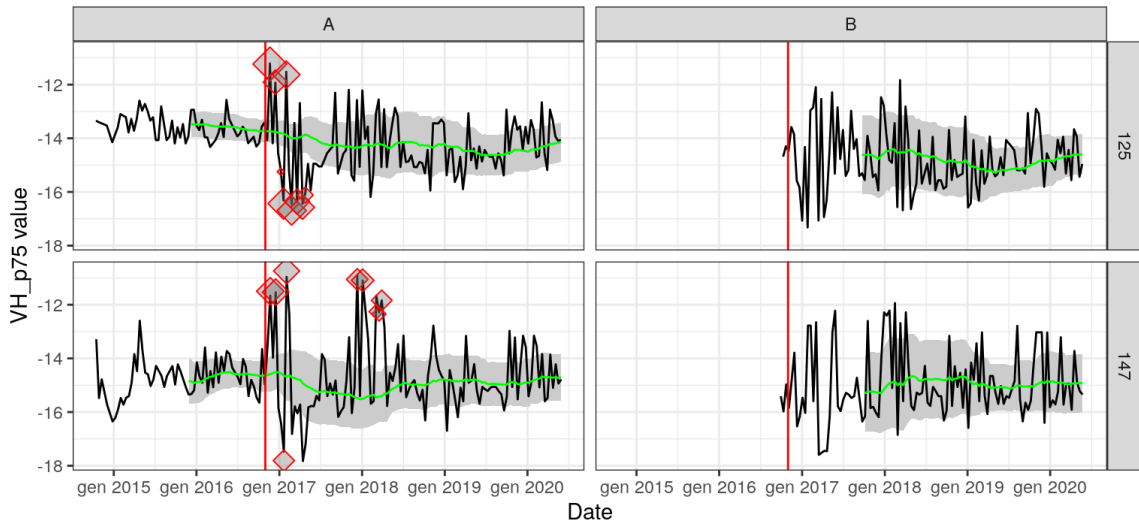
Area: PF16_1 - Variable: VH_p25 - Z-score > 3



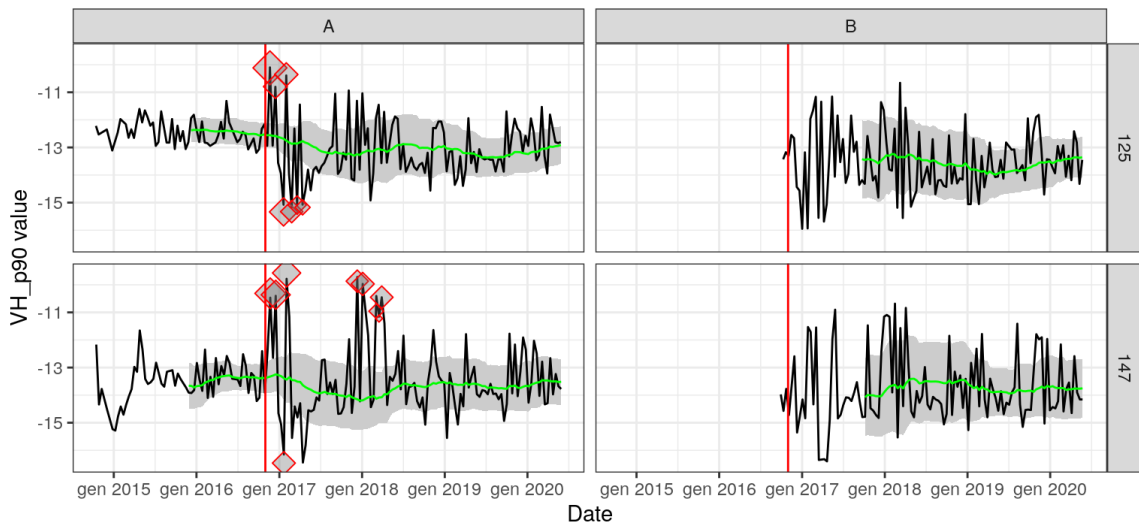
Area: PF16_1 - Variable: VH_p50 - Z-score > 3



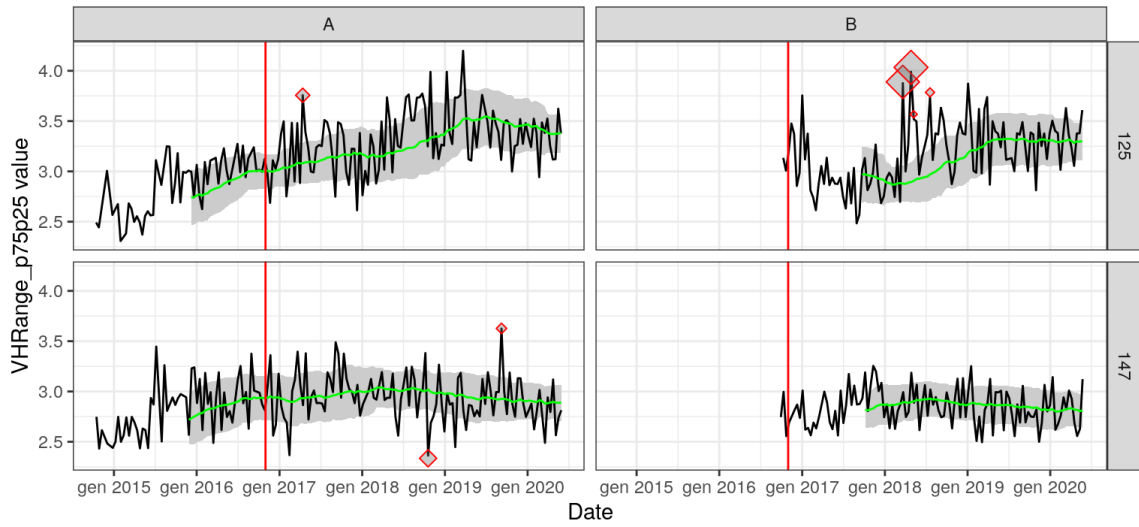
Area: PF16_1 - Variable: VH_p75 - Z-score > 3



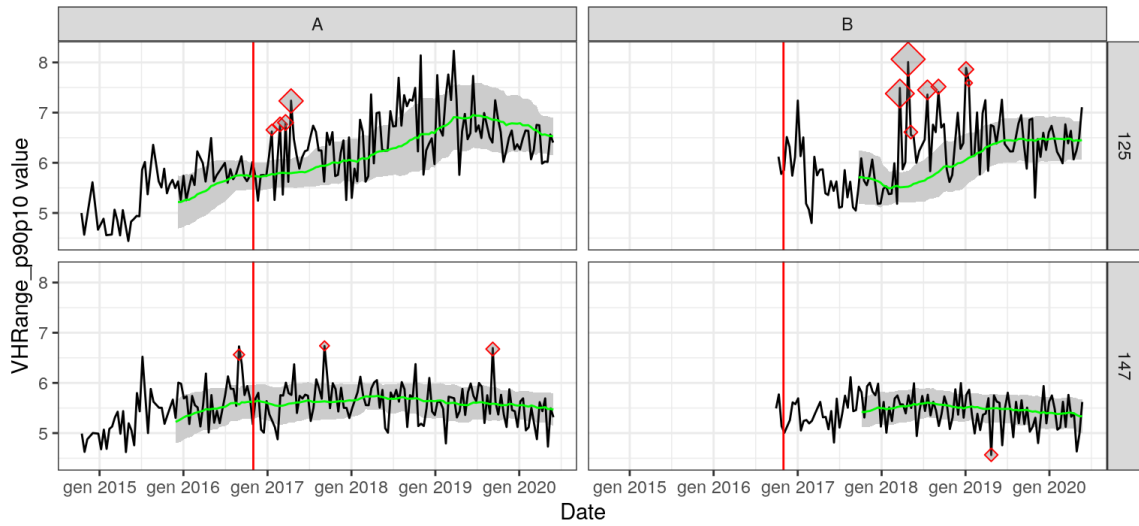
Area: PF16_1 - Variable: VH_p90 - Z-score > 3



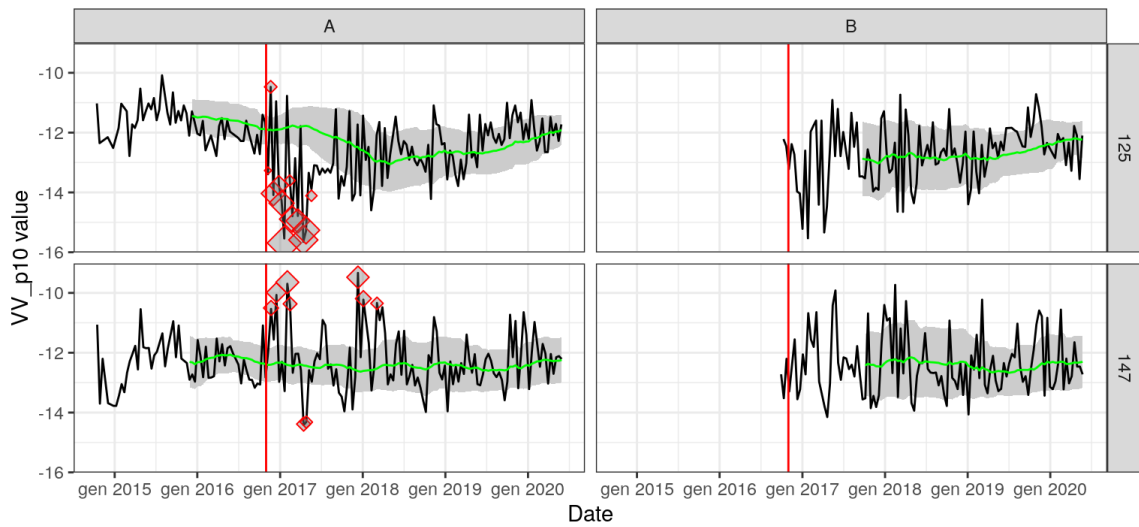
Area: PF16_1 - Variable: VHRange_p75p25 - Z-score > 3



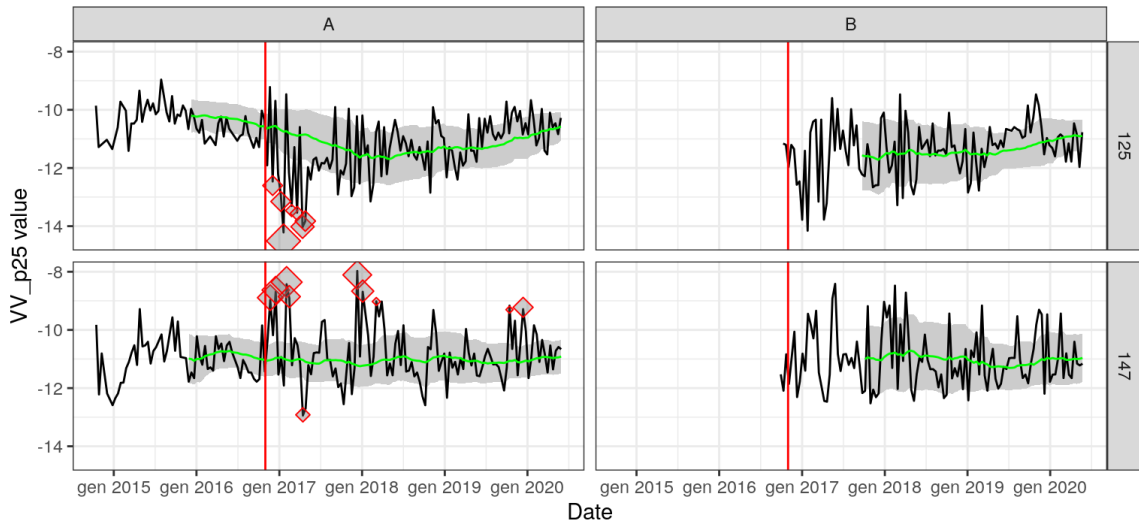
Area: PF16_1 - Variable: VHRange_p90p10 - Z-score > 3



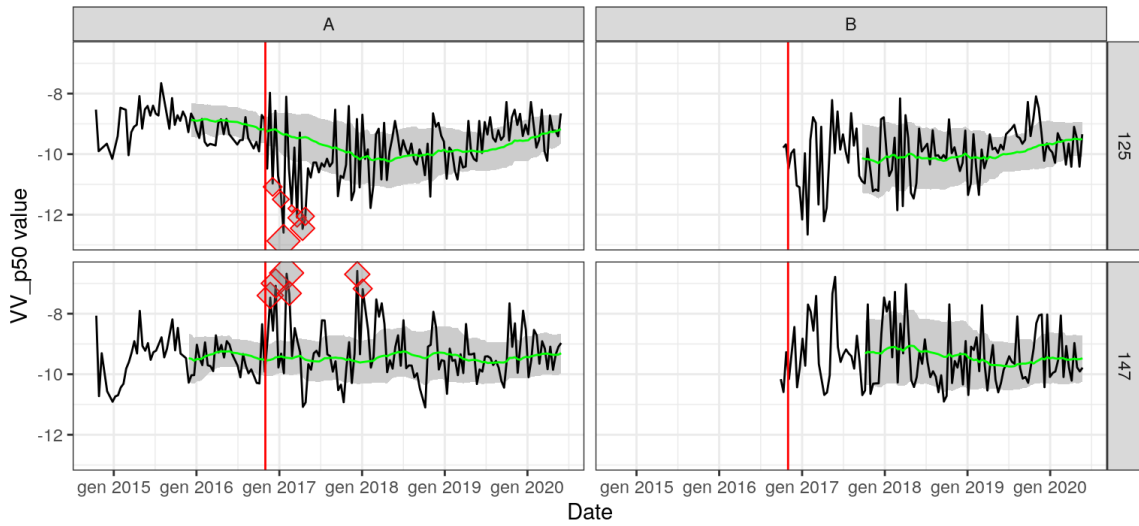
Area: PF16_1 - Variable: VV_p10 - Z-score > 3



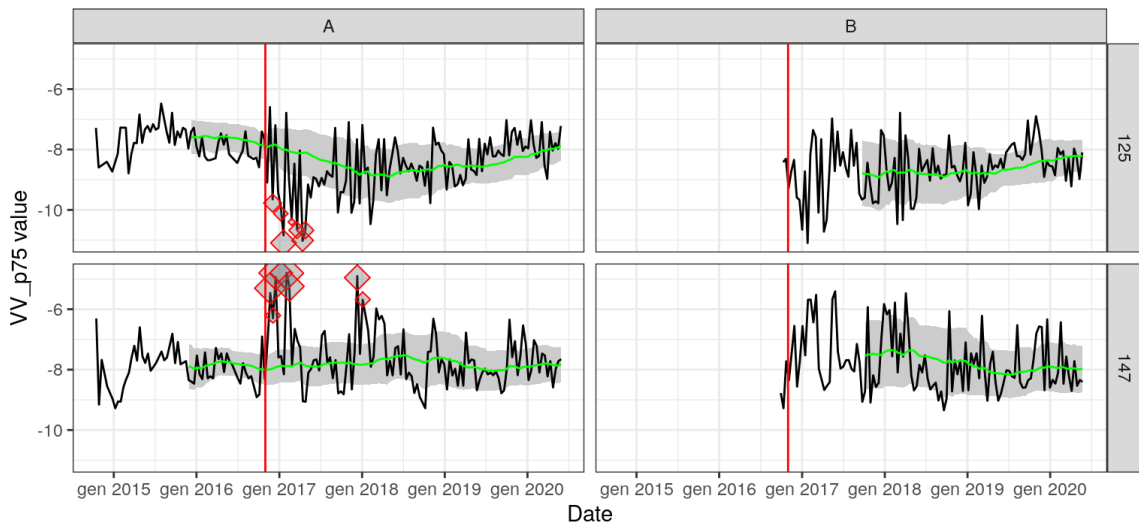
Area: PF16_1 - Variable: VV_p25 - Z-score > 3



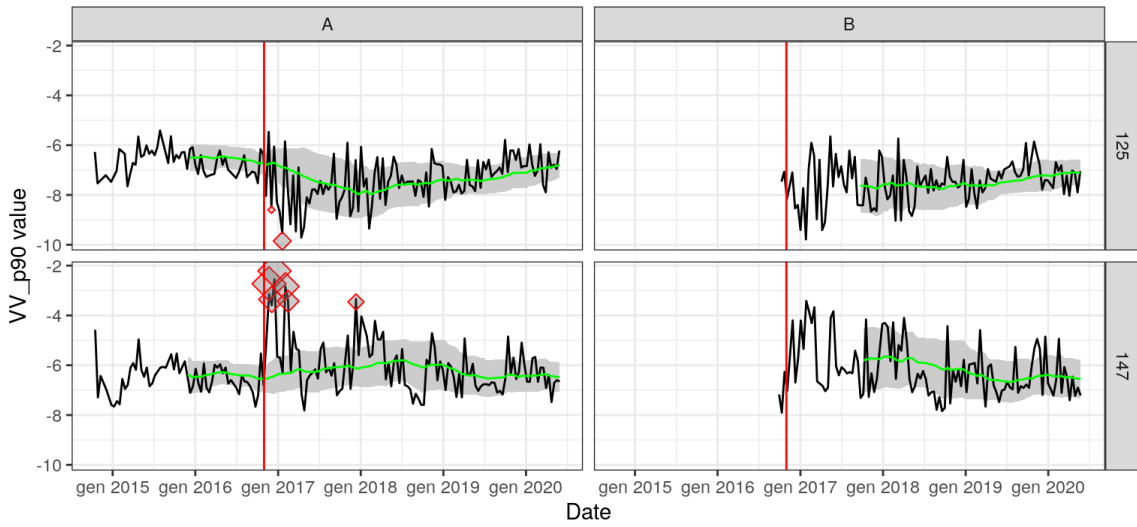
Area: PF16_1 - Variable: VV_p50 - Z-score > 3



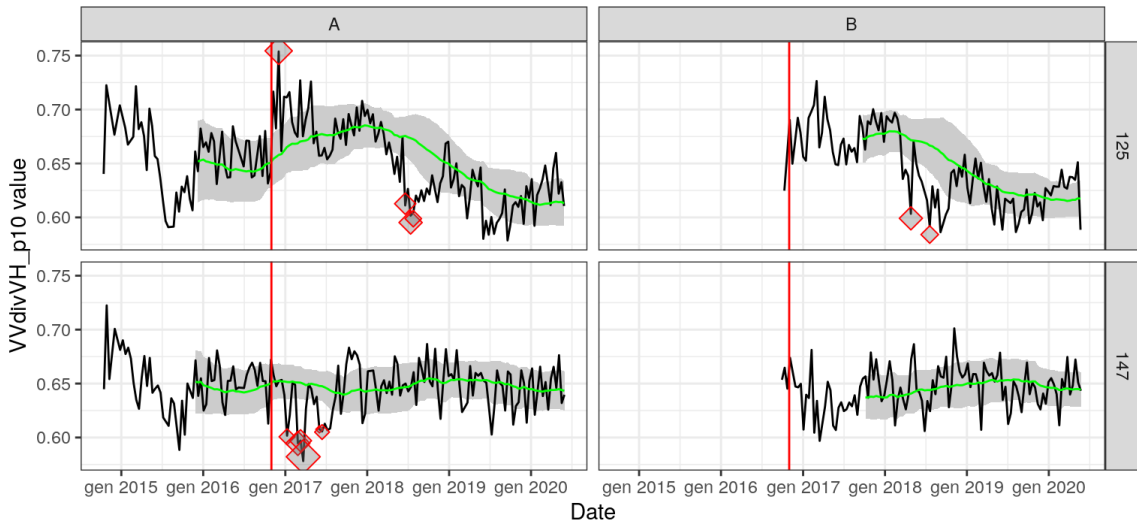
Area: PF16_1 - Variable: VV_p75 - Z-score > 3



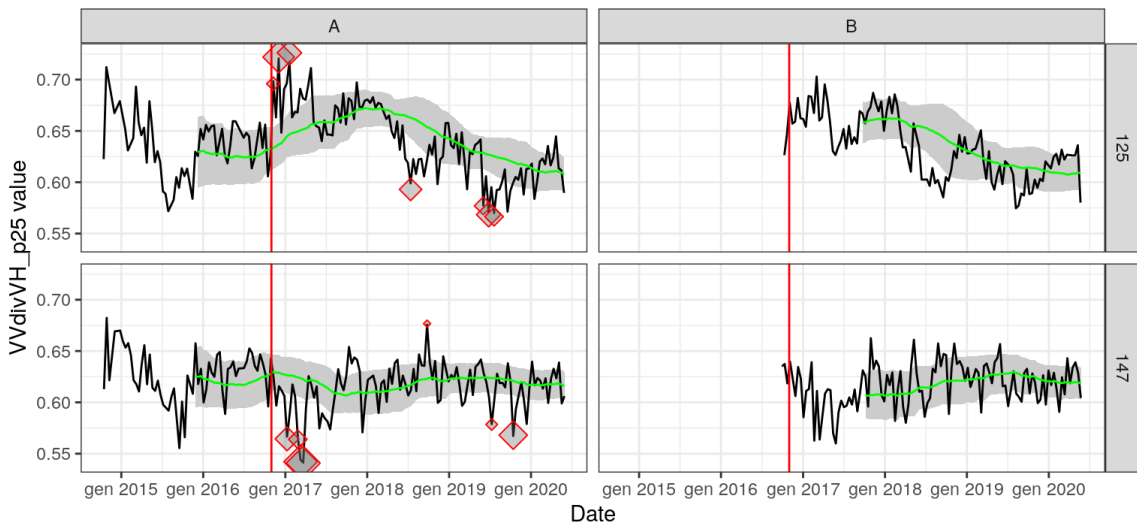
Area: PF16_1 - Variable: VV_p90 - Z-score > 3



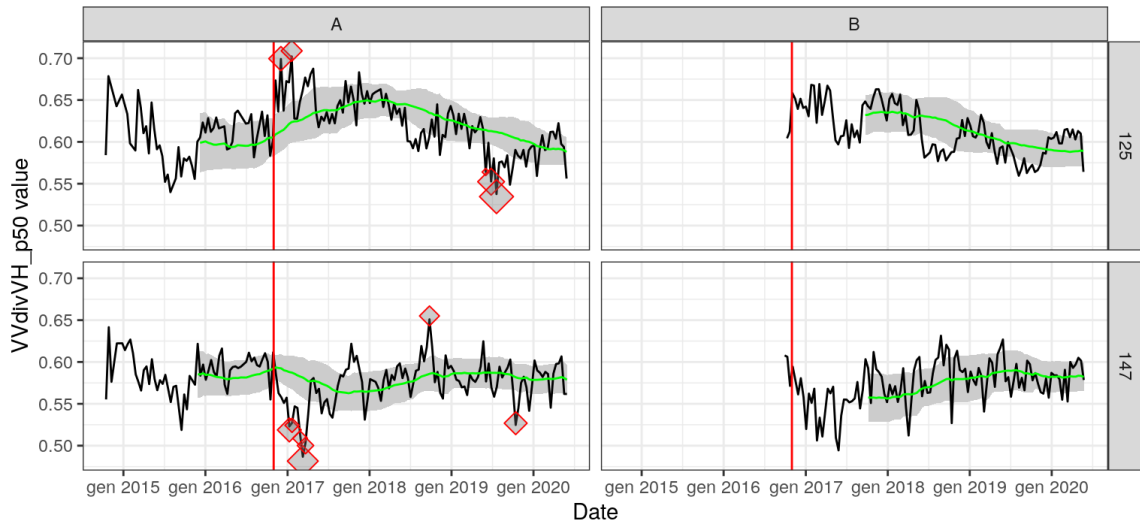
Area: PF16_1 - Variable: VVdivVH_p10 - Z-score > 3



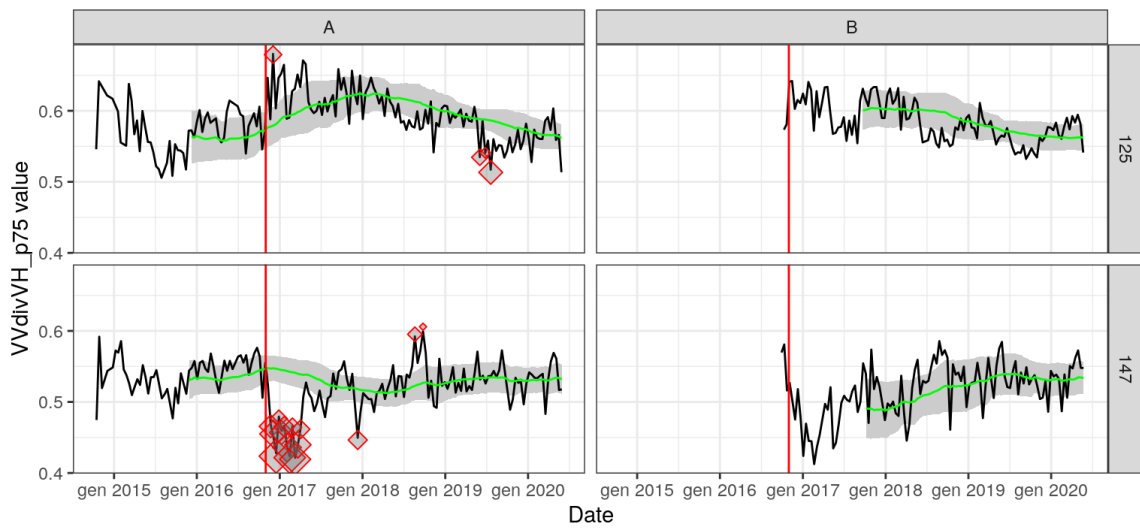
Area: PF16_1 - Variable: VVdivVH_p25 - Z-score > 3



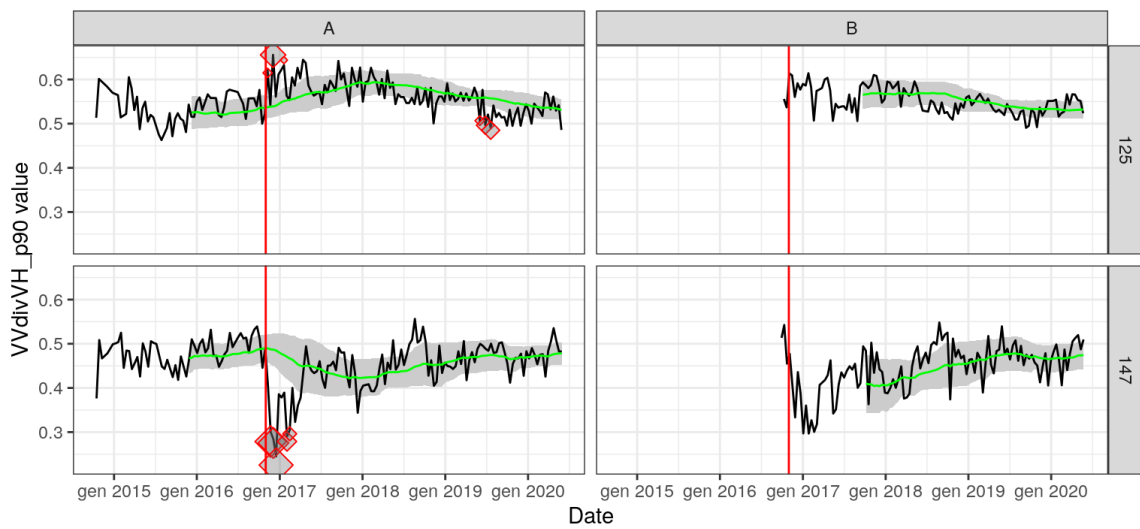
Area: PF16_1 - Variable: VVdivVH_p50 - Z-score > 3



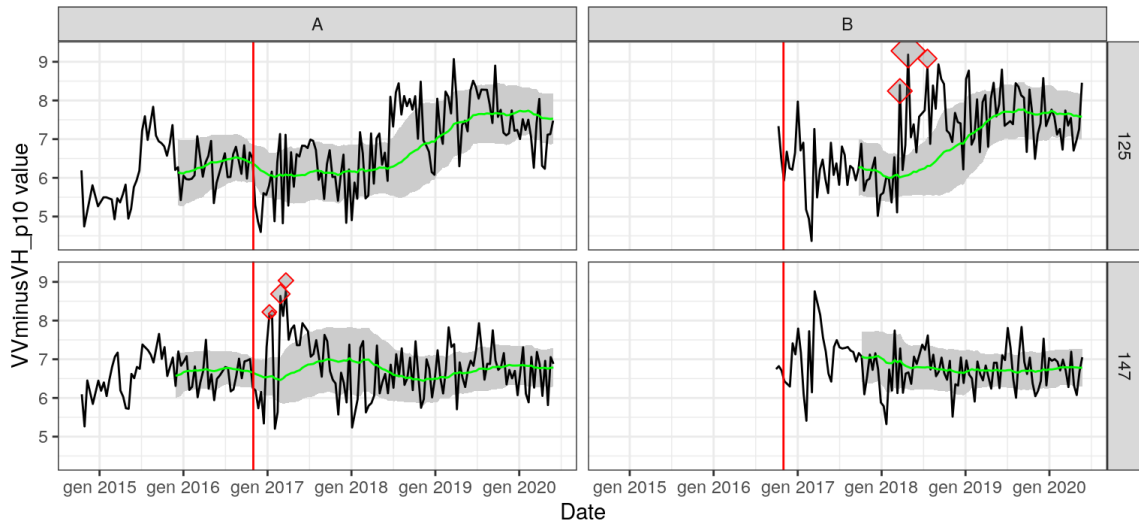
Area: PF16_1 - Variable: VVdivVH_p75 - Z-score > 3



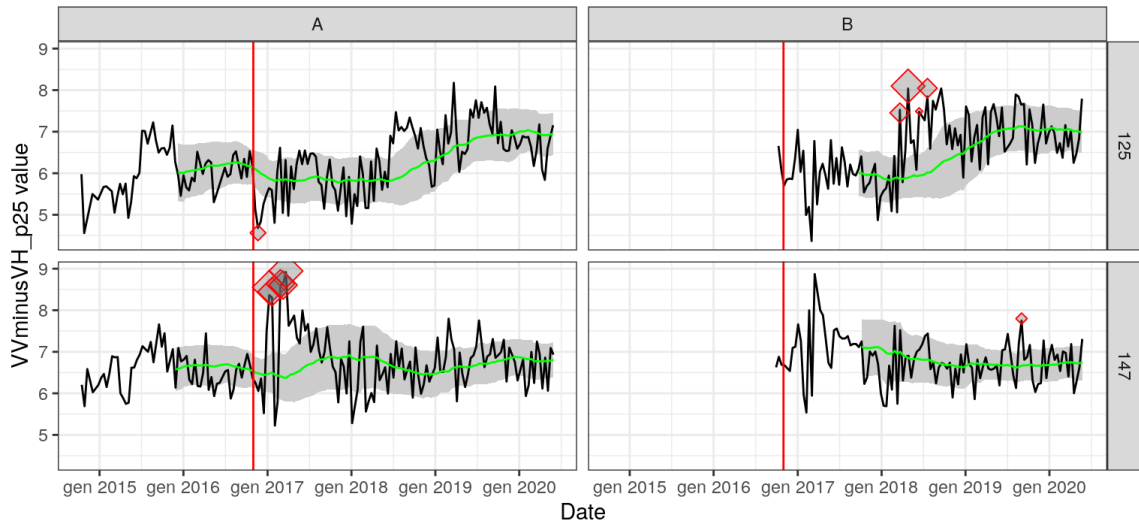
Area: PF16_1 - Variable: VVdivVH_p90 - Z-score > 3



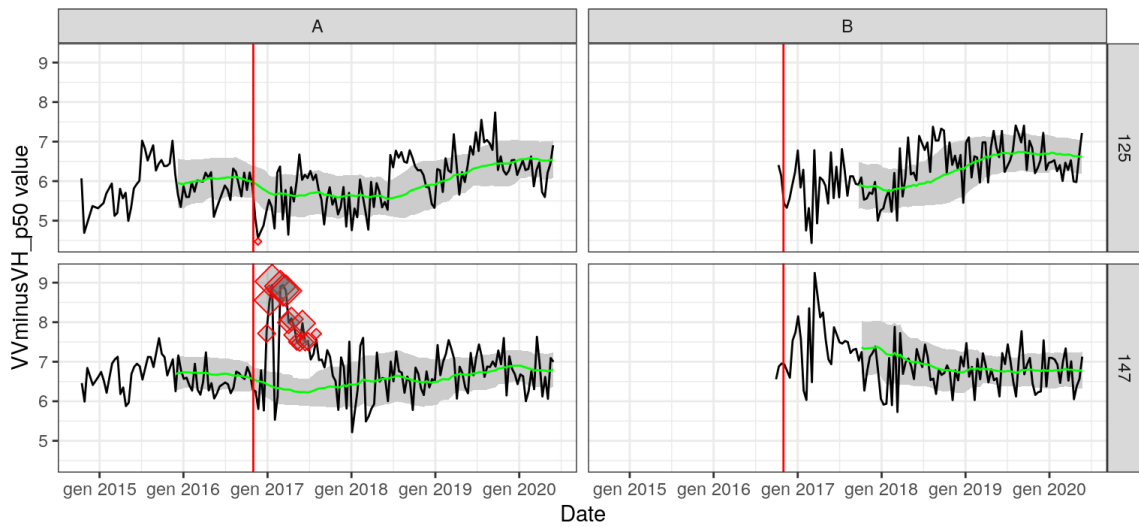
Area: PF16_1 - Variable: VVminusVH_p10 - Z-score > 3



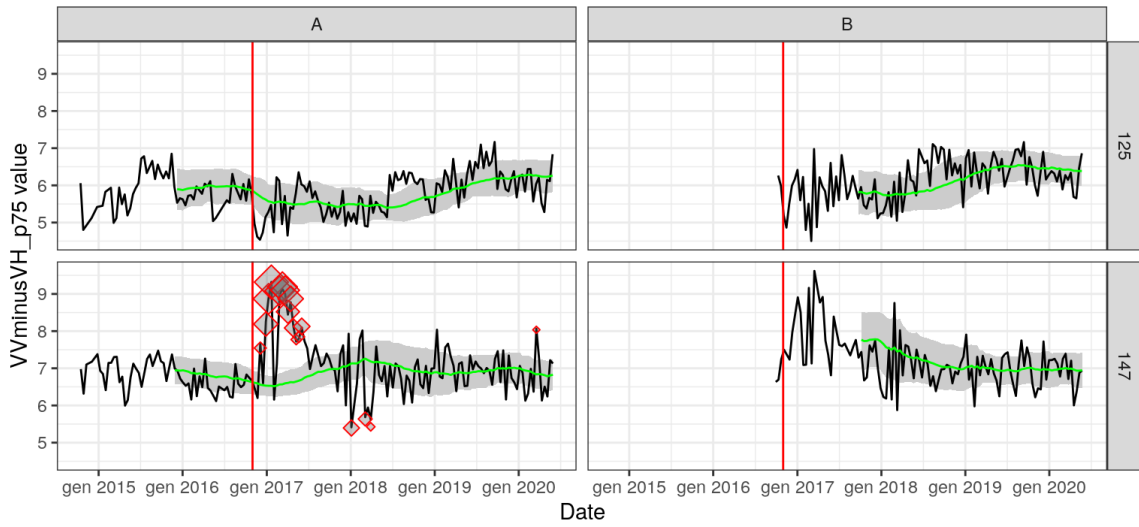
Area: PF16_1 - Variable: VVminusVH_p25 - Z-score > 3



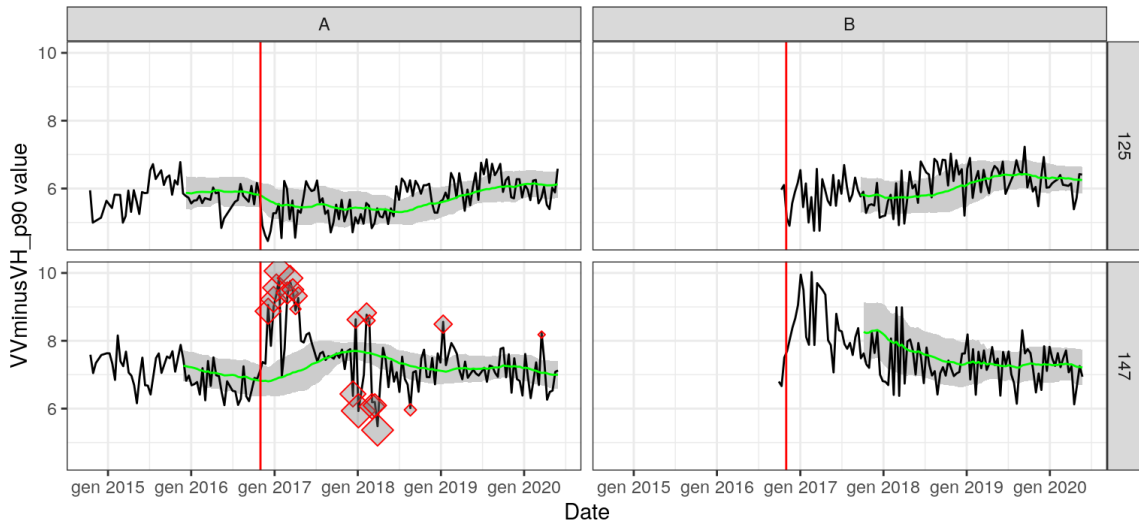
Area: PF16_1 - Variable: VVminusVH_p50 - Z-score > 3



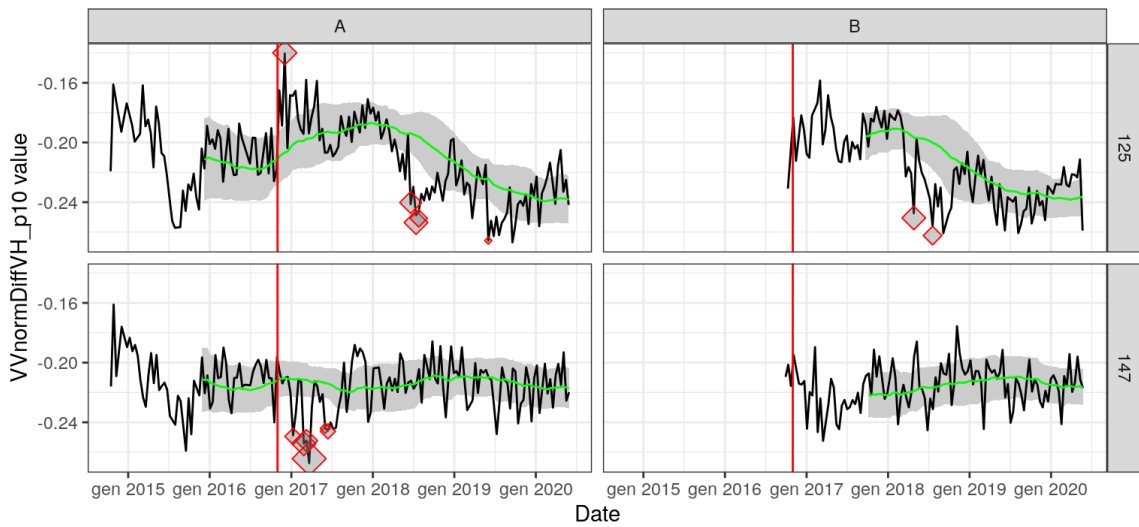
Area: PF16_1 - Variable: VVminusVH_p75 - Z-score > 3



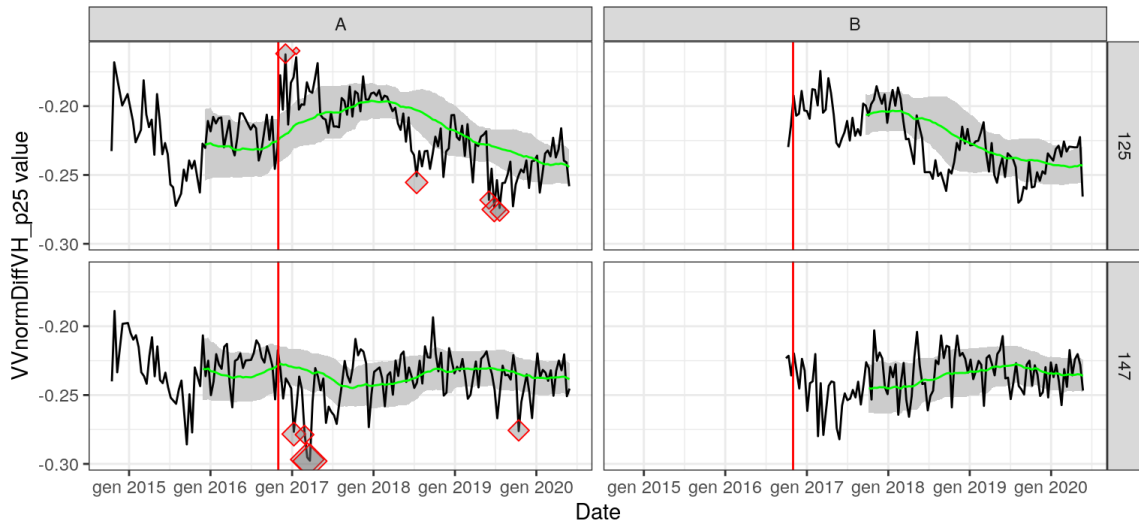
Area: PF16_1 - Variable: VVminusVH_p90 - Z-score > 3



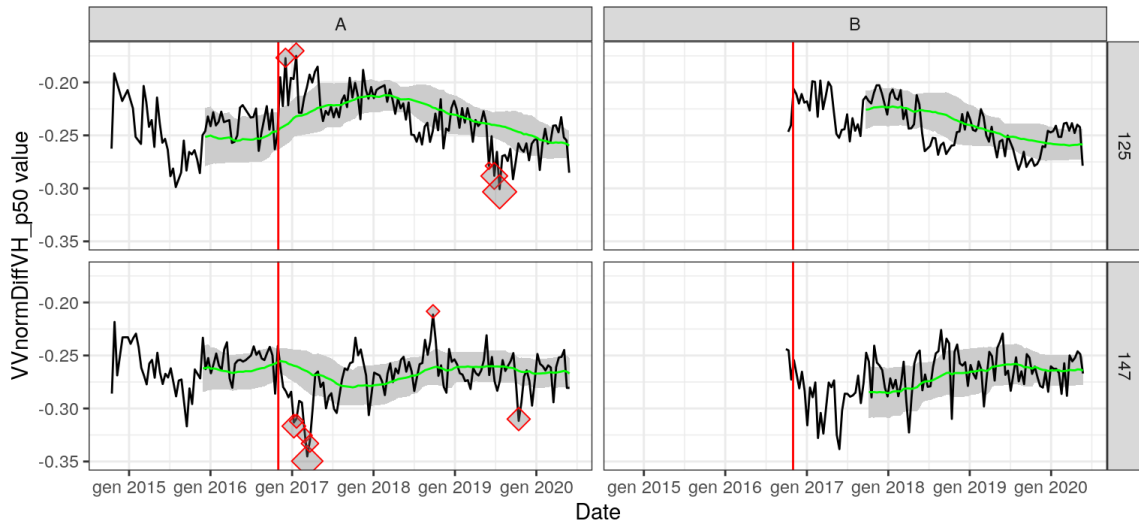
Area: PF16_1 - Variable: VVnormDiffVH_p10 - Z-score > 3



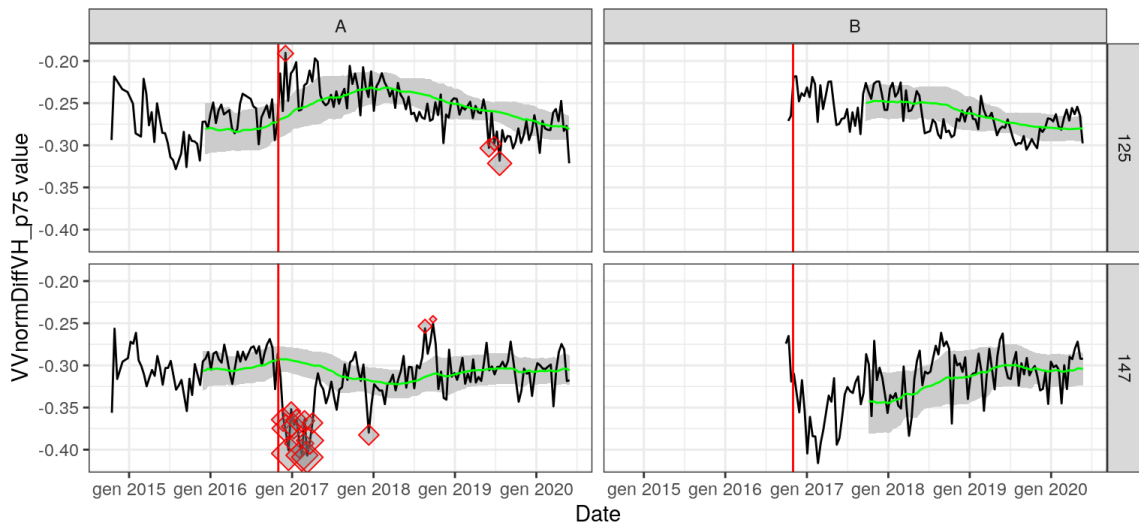
Area: PF16_1 - Variable: VVnormDiffVH_p25 - Z-score > 3



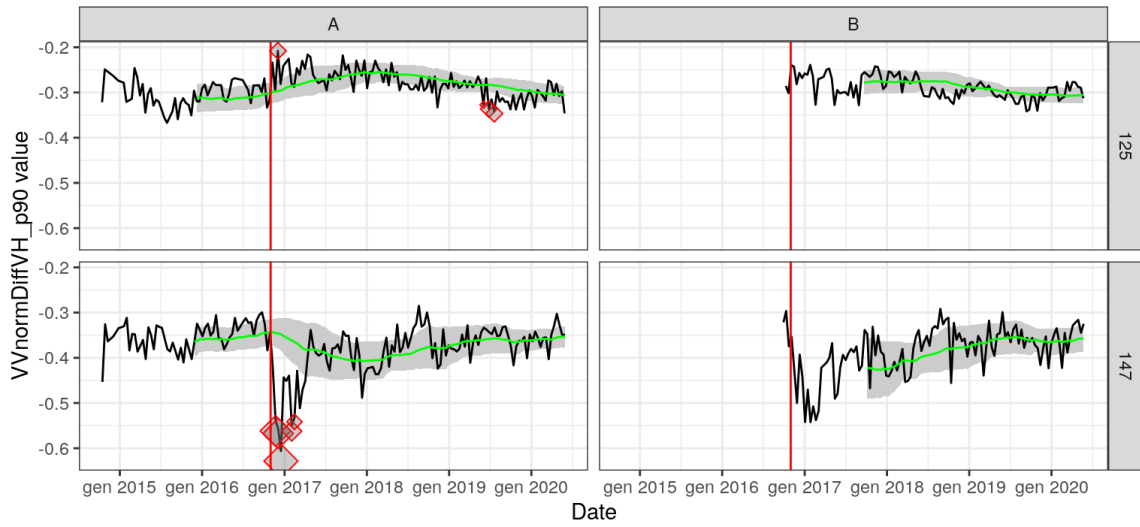
Area: PF16_1 - Variable: VVnormDiffVH_p50 - Z-score > 3



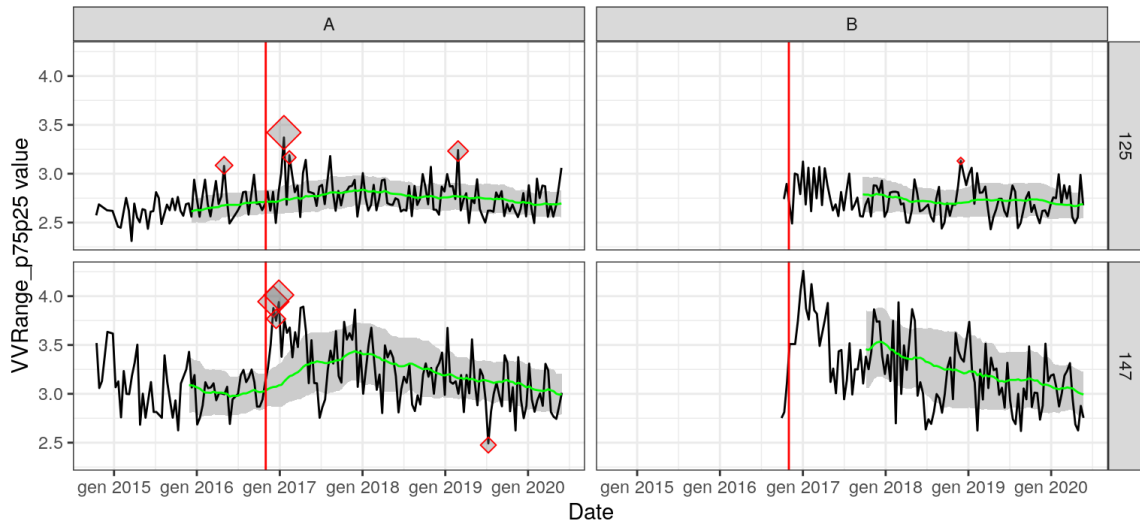
Area: PF16_1 - Variable: VVnormDiffVH_p75 - Z-score > 3



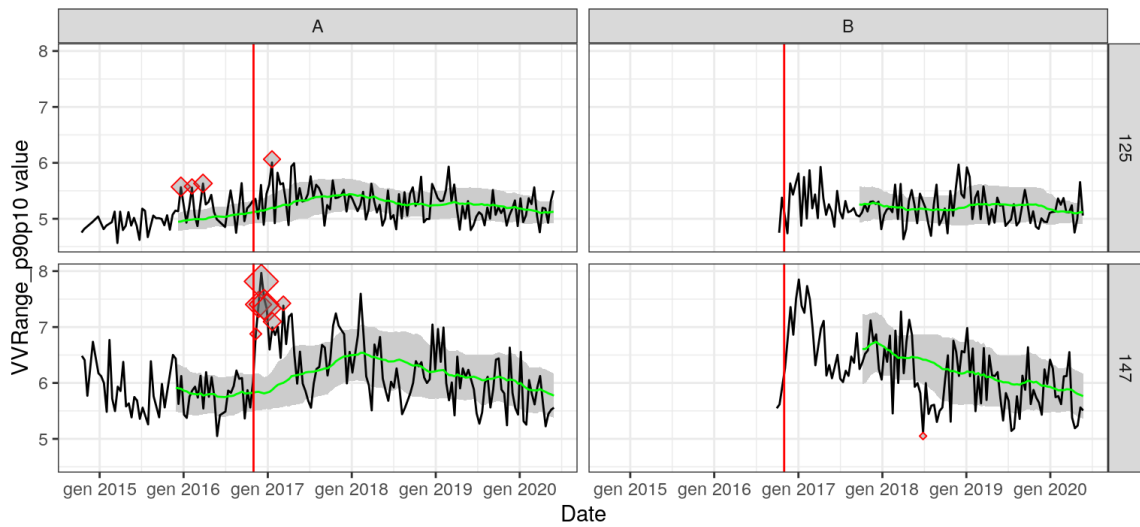
Area: PF16_1 - Variable: VVnormDiffVH_p90 - Z-score > 3



Area: PF16_1 - Variable: VVRange_p75p25 - Z-score > 3

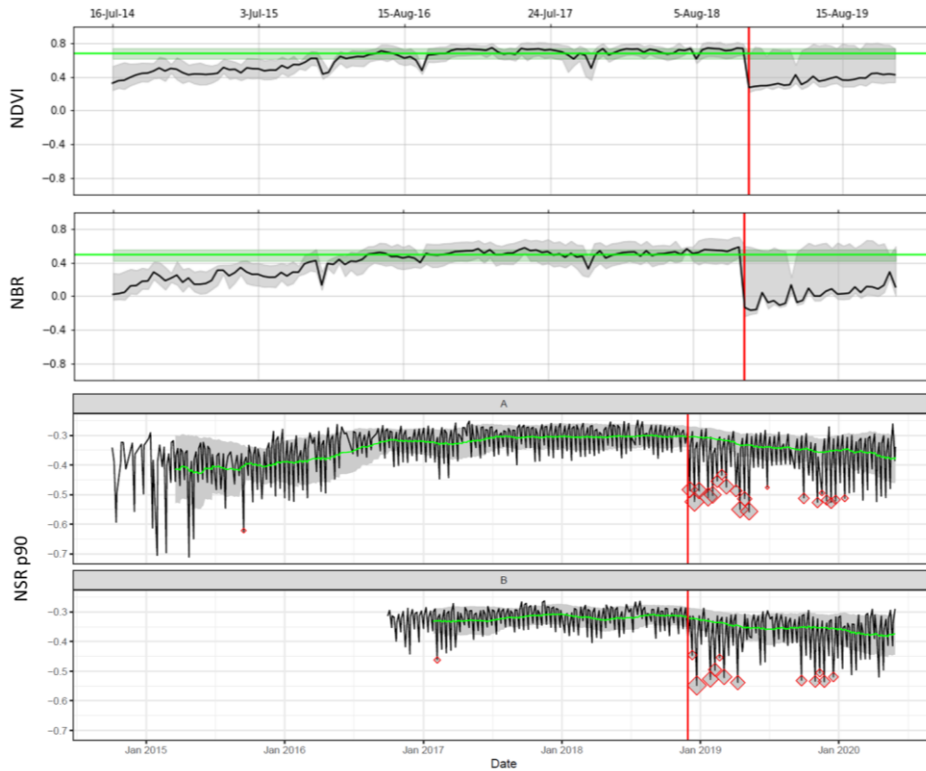


Area: PF16_1 - Variable: VVRange_p90p10 - Z-score > 3

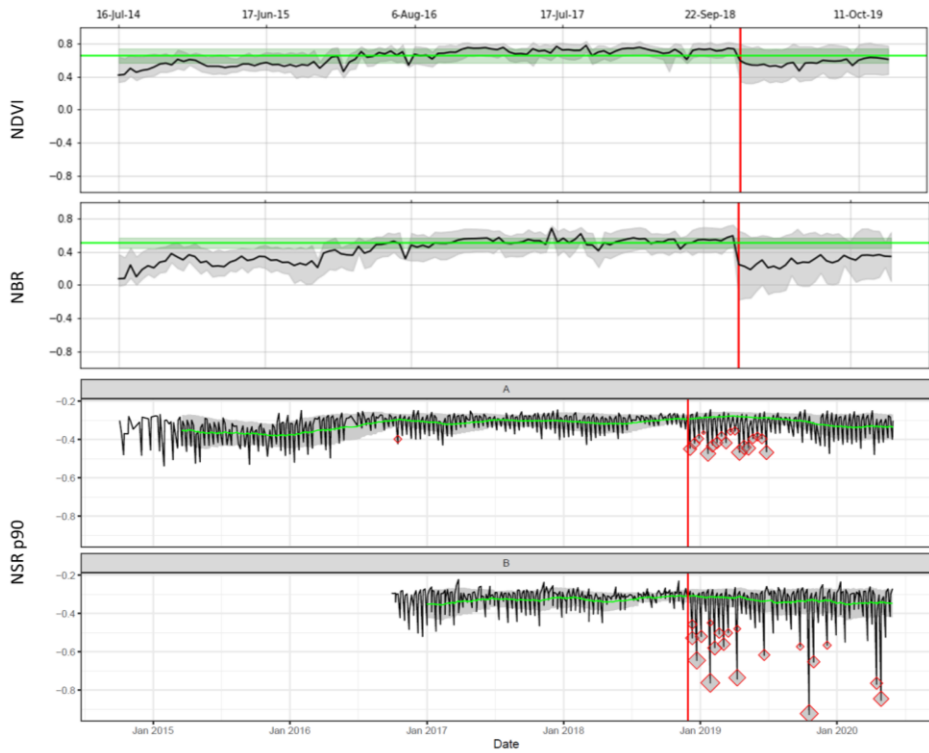


Appendix 2 – Spectral Indices and SAR comparison

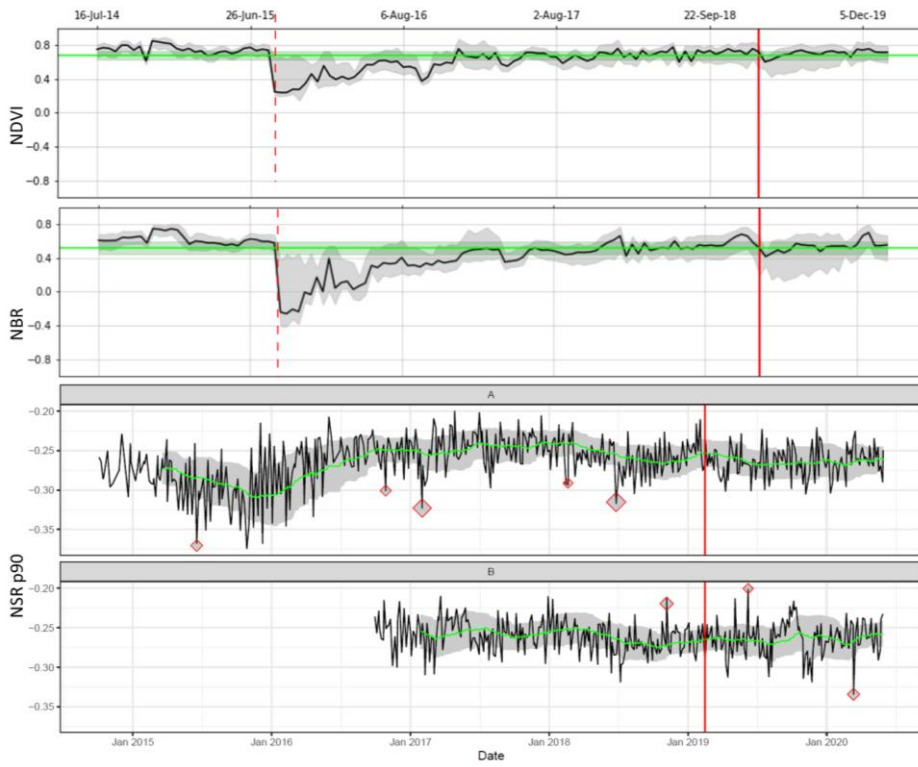
Prescribed Fires 2018_1



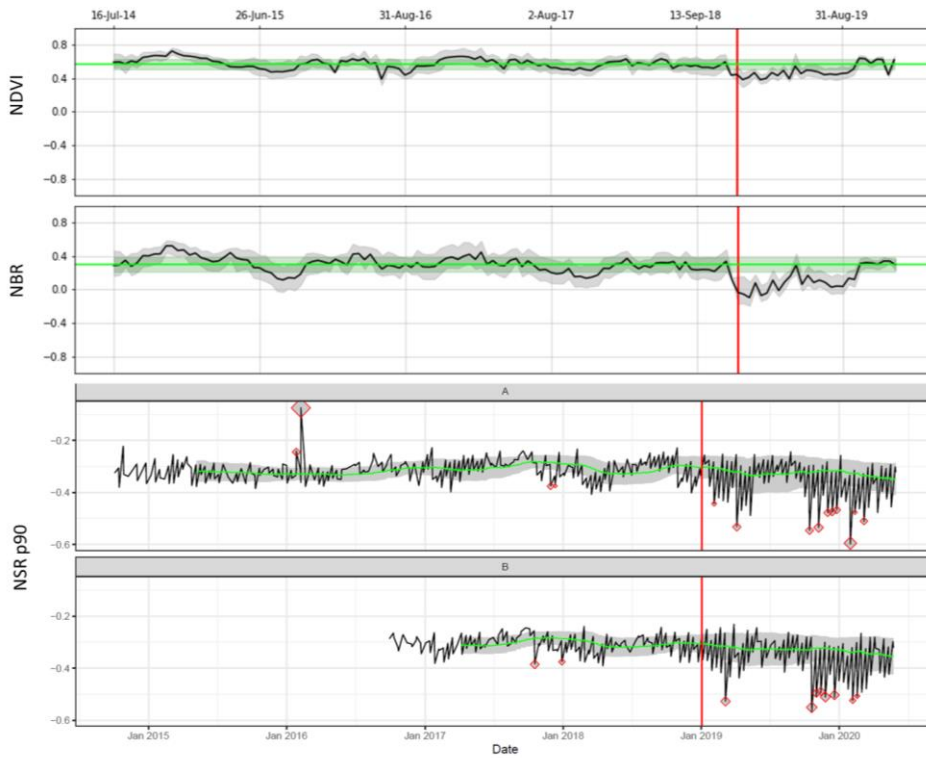
Prescribed Fire 2018_2



Prescribed Fire 2019_6



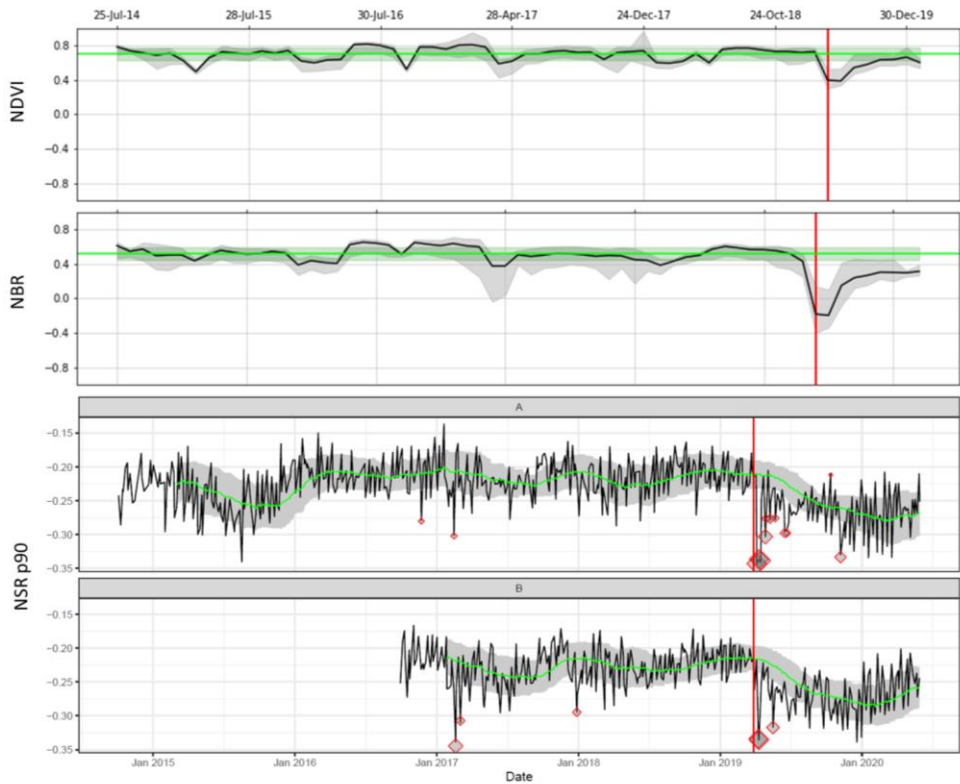
Prescribed Fire 2019_8



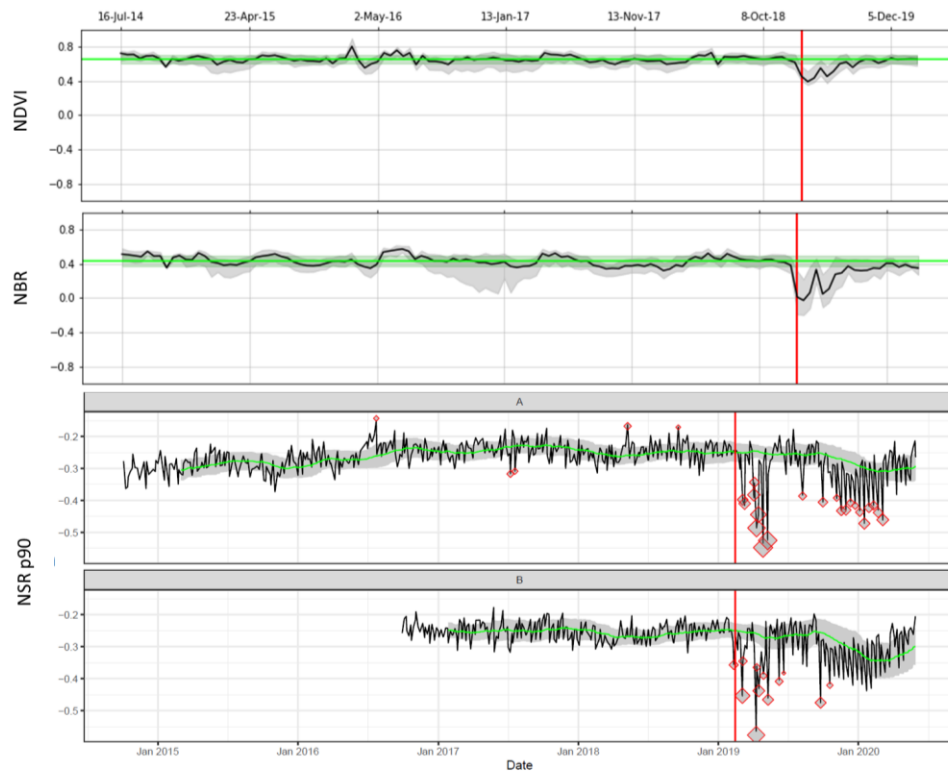
Prescribed Fire 2019_11



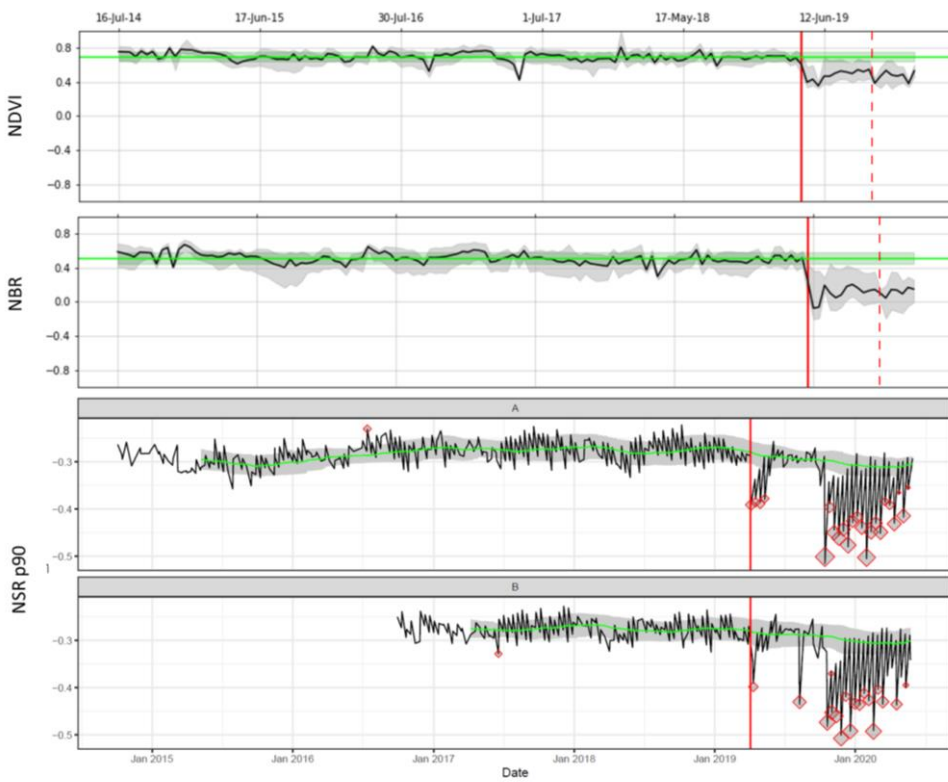
Prescribed Fires 2019_12



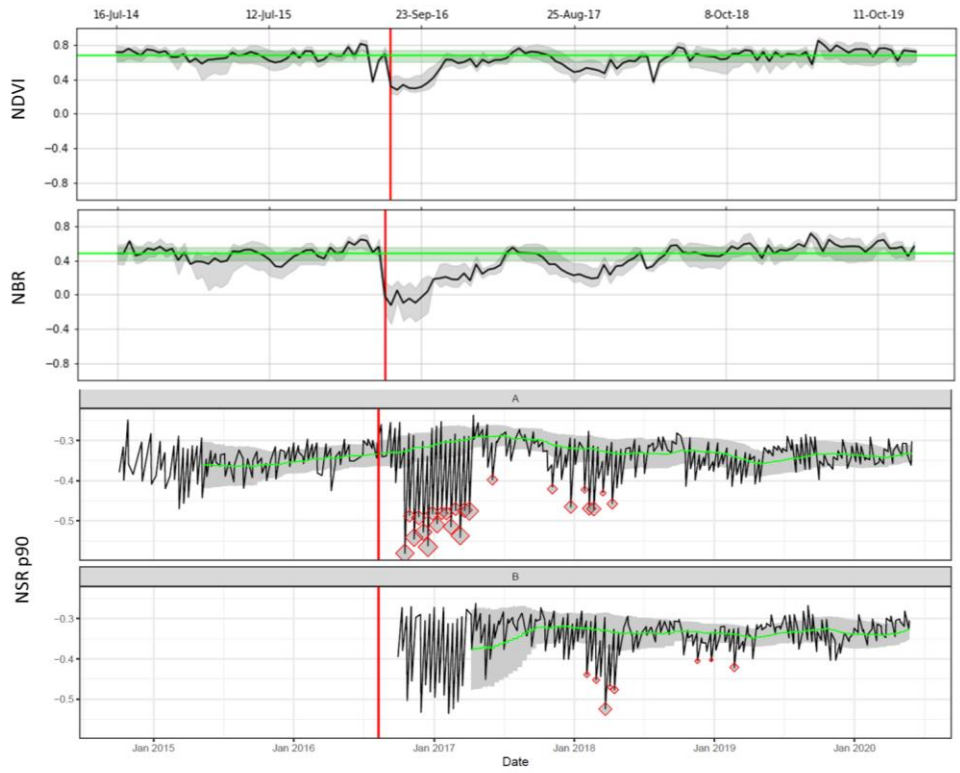
Prescribed Fires 2019_13



Prescribed Fires 2019_15



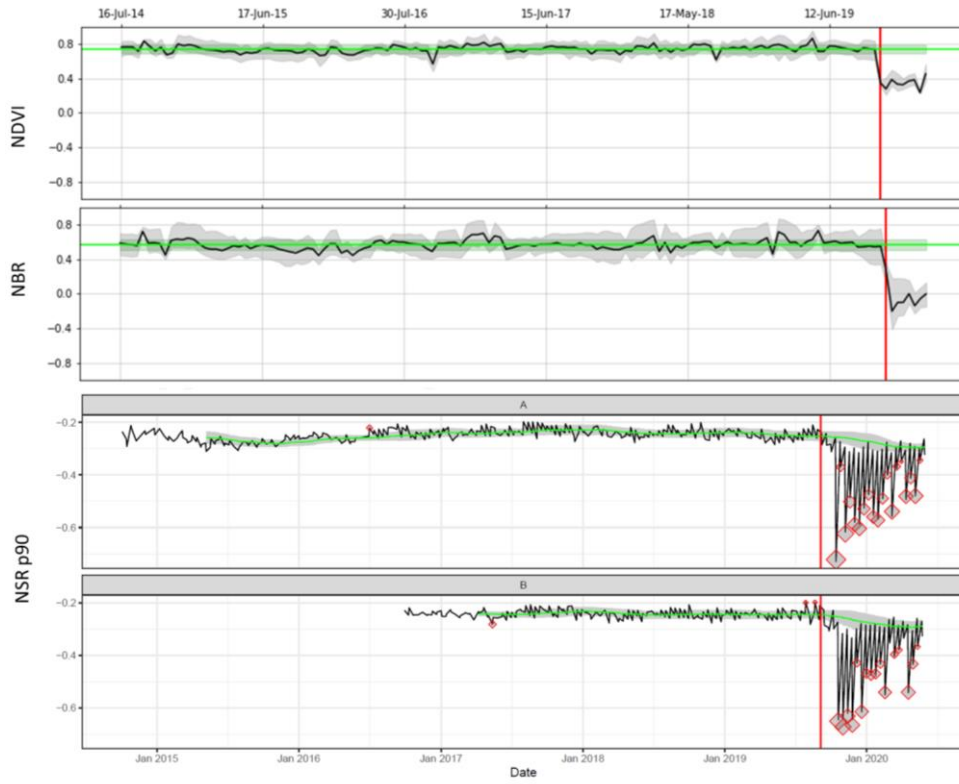
Summer Wildfire 2016_1



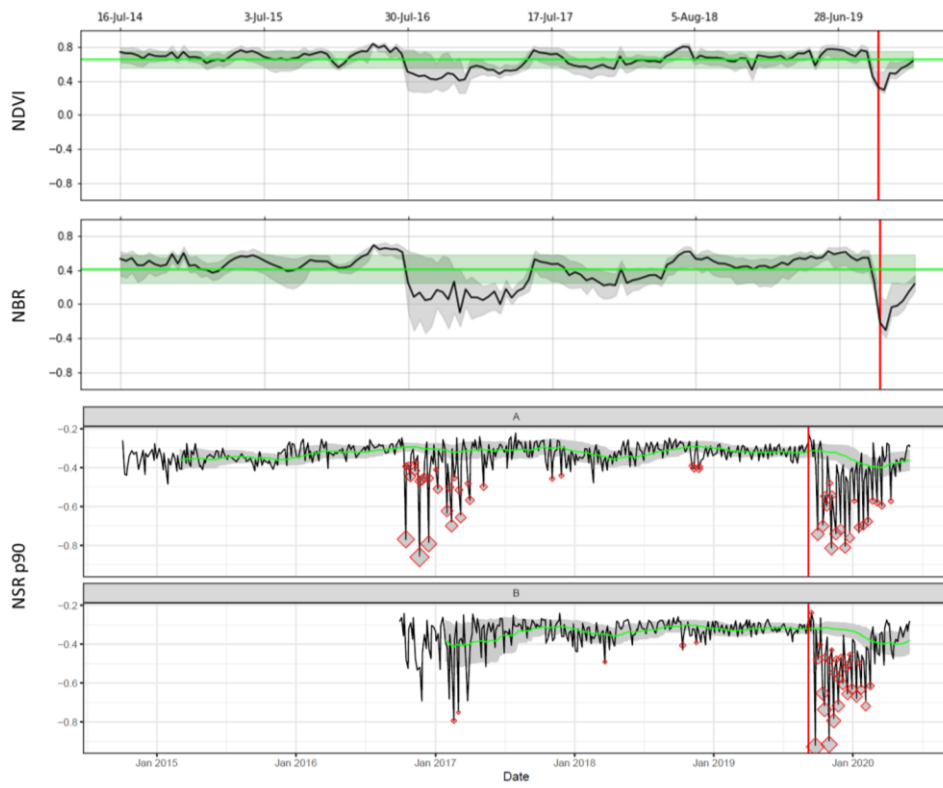
Summer Wildfire 2019_6



Summer Wildfires 2019_15



Summer Wildfire 2019_18



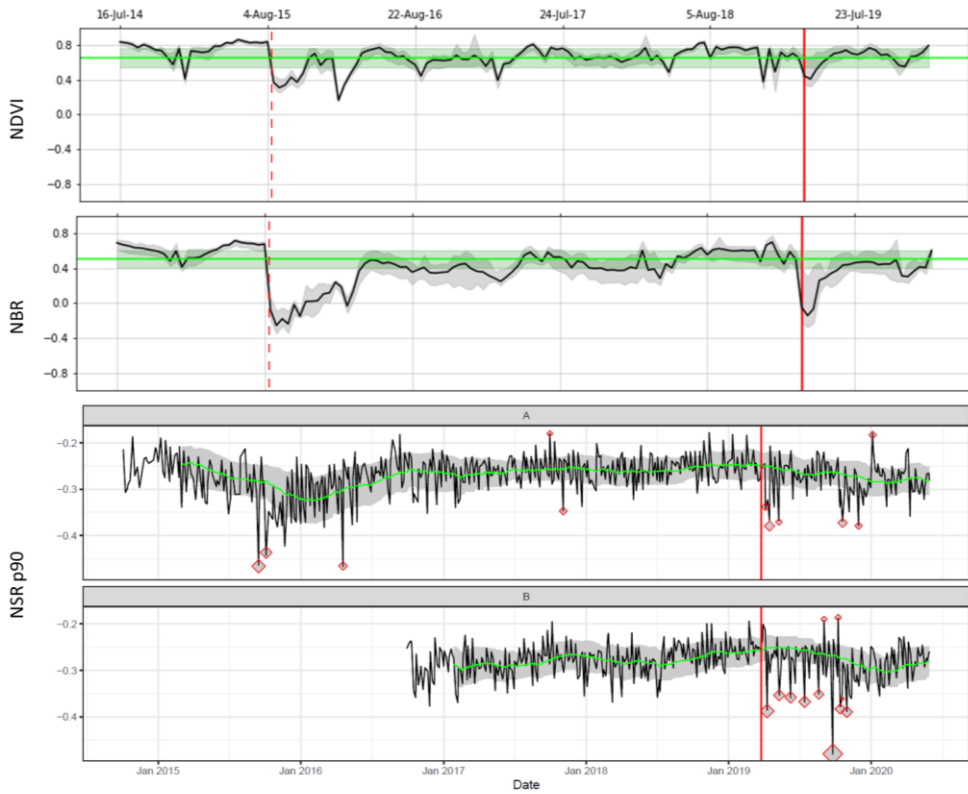
Winter Wildfire 2018_1



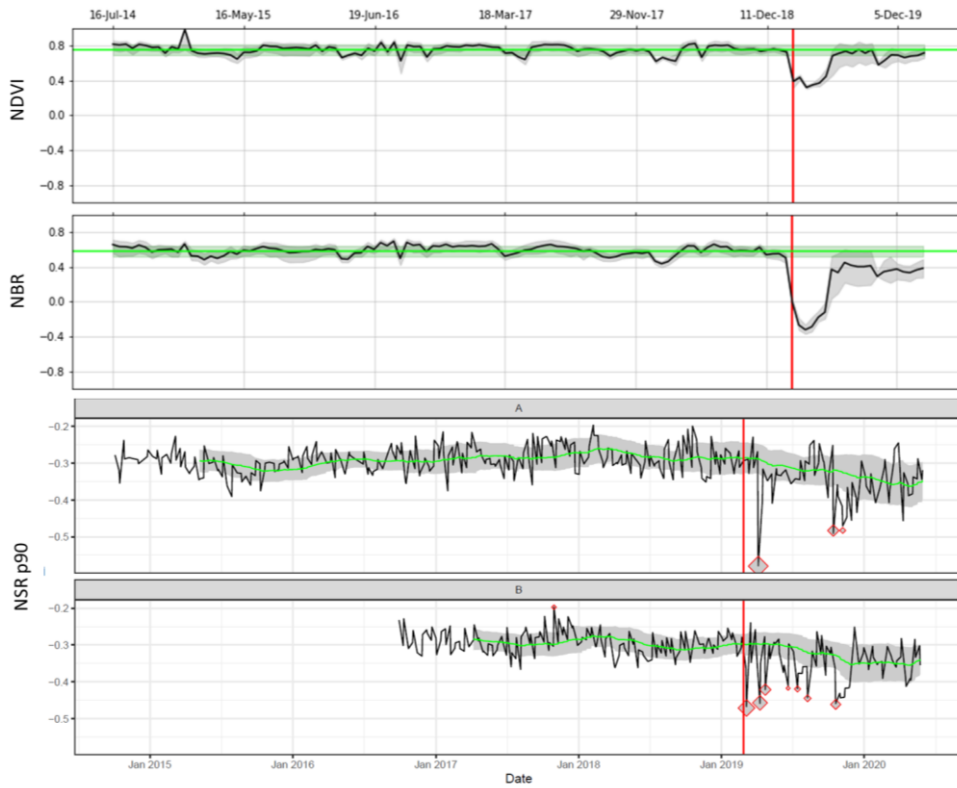
Winter Wildfire 2018_2



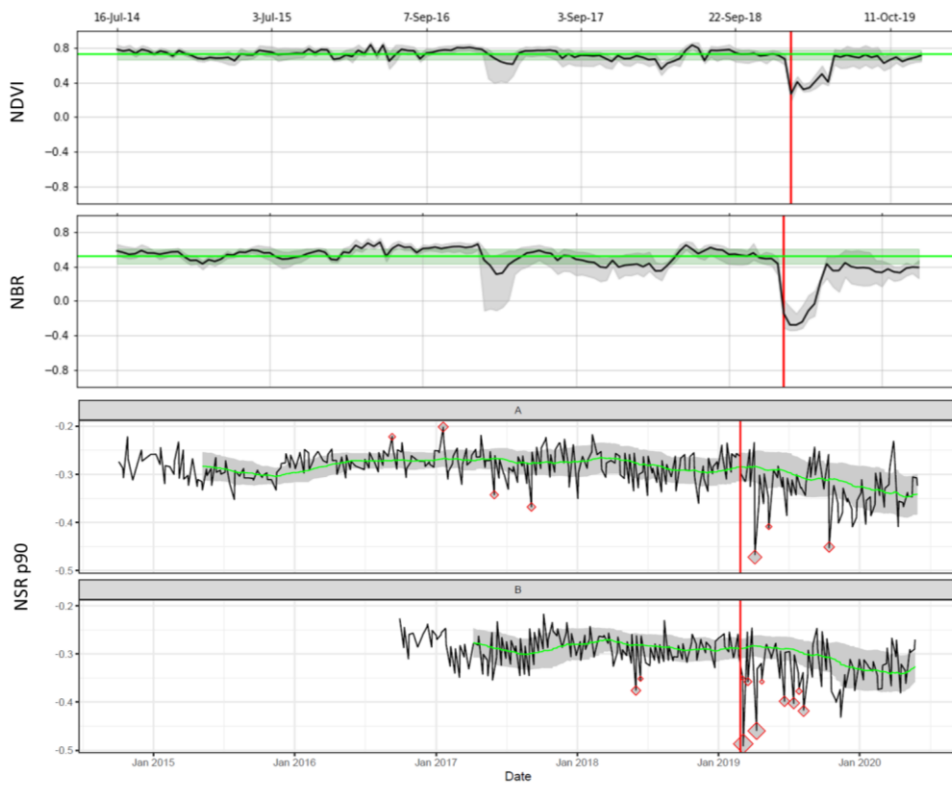
Winter Wildfire 2019_6



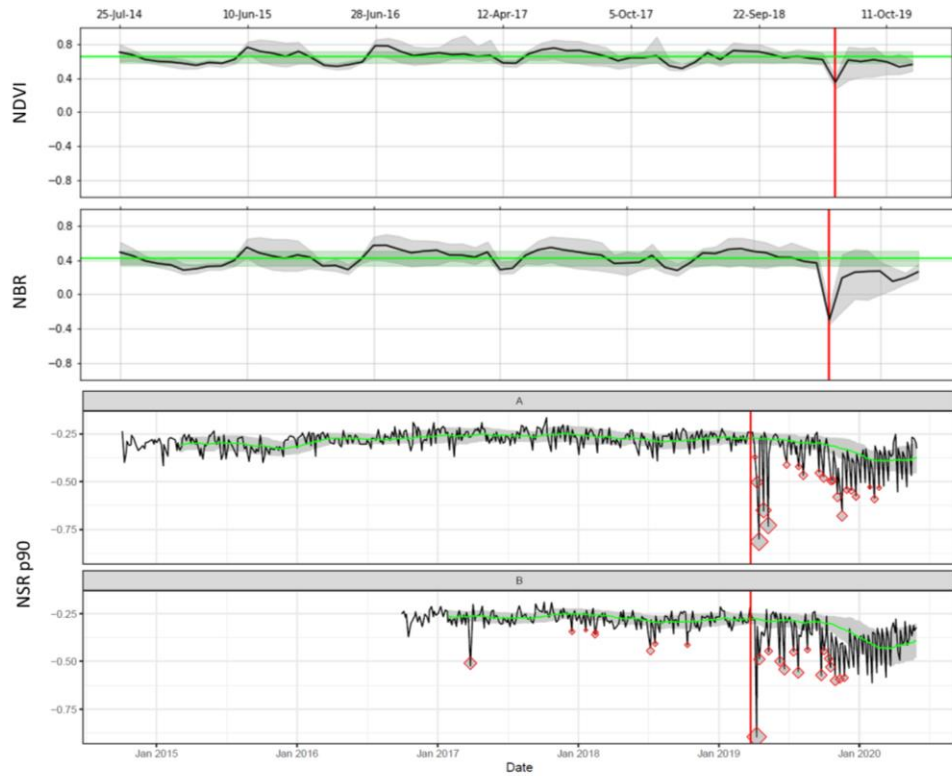
Winter Wildfire 2019_8



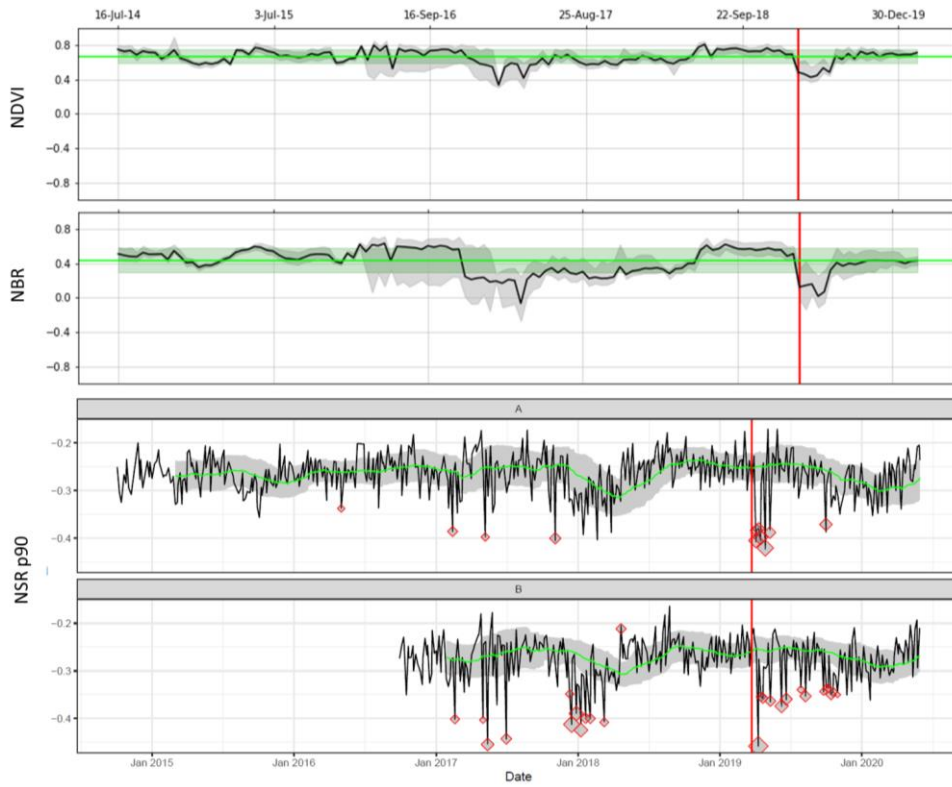
Winter Wildfire 2019_11



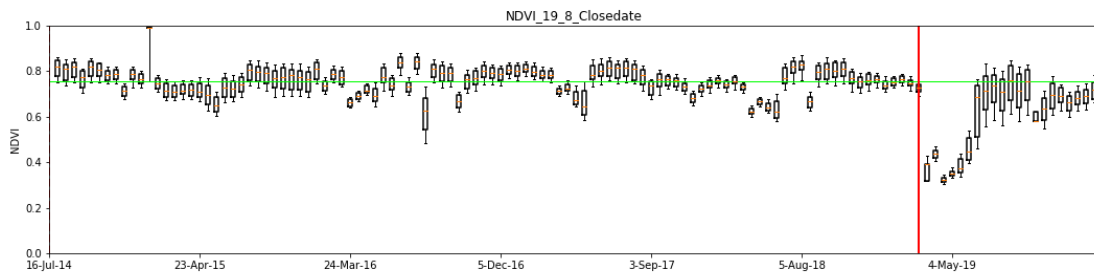
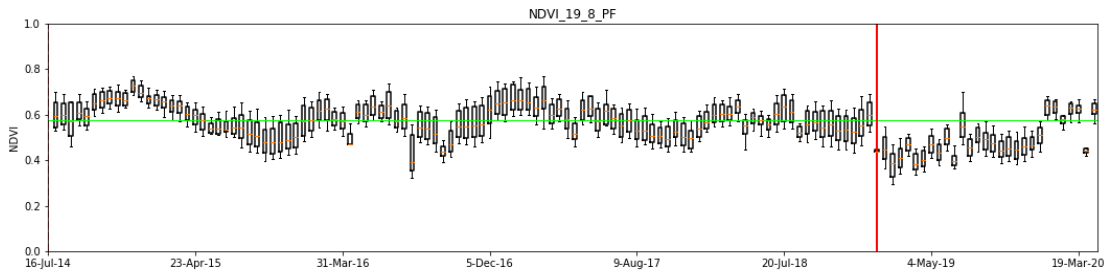
Winter Wildfires 2019_12

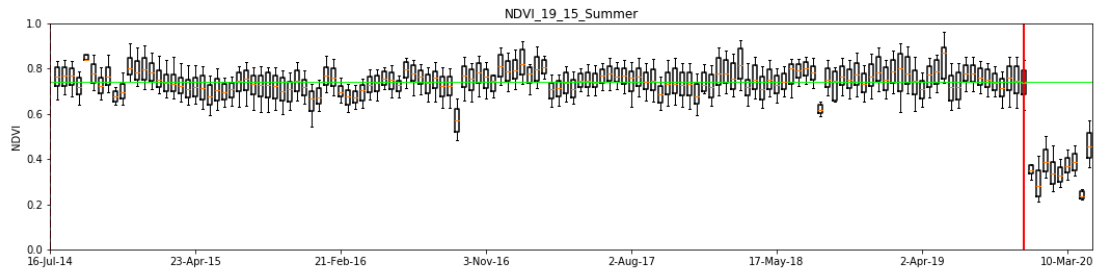
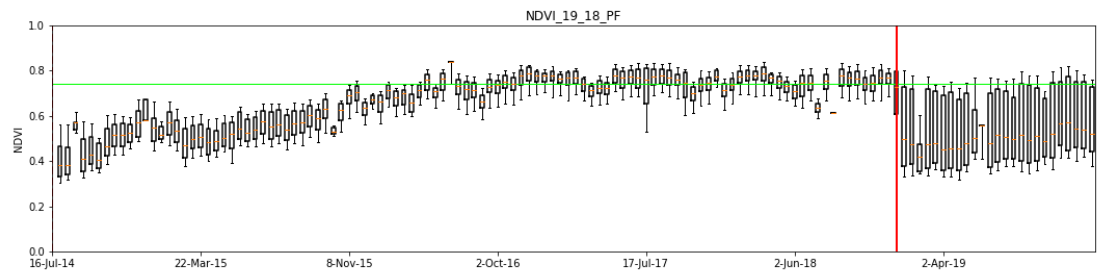
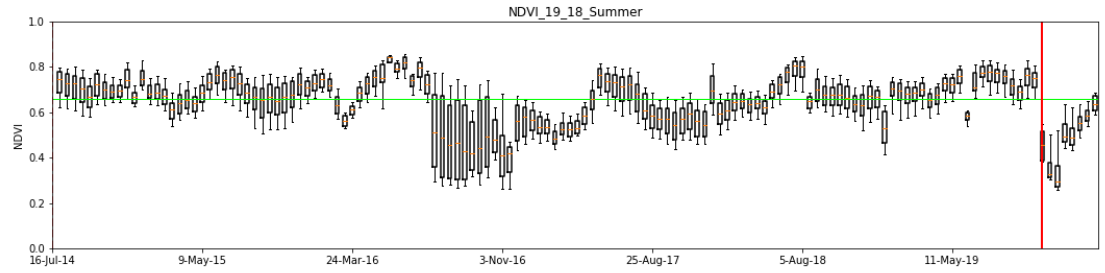
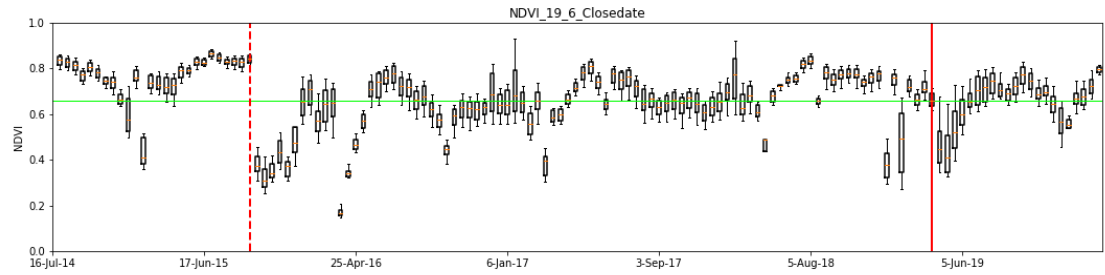
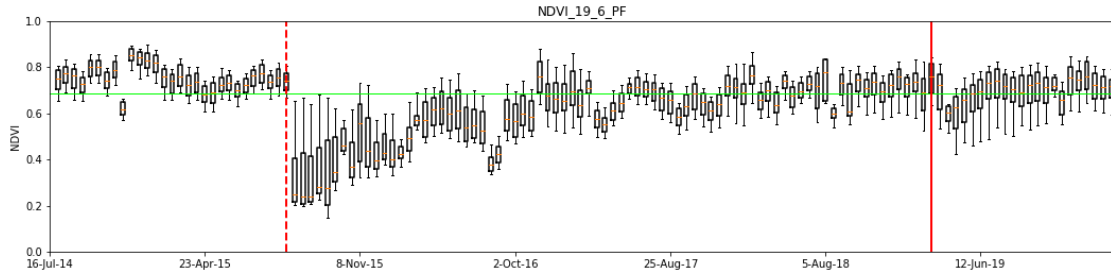
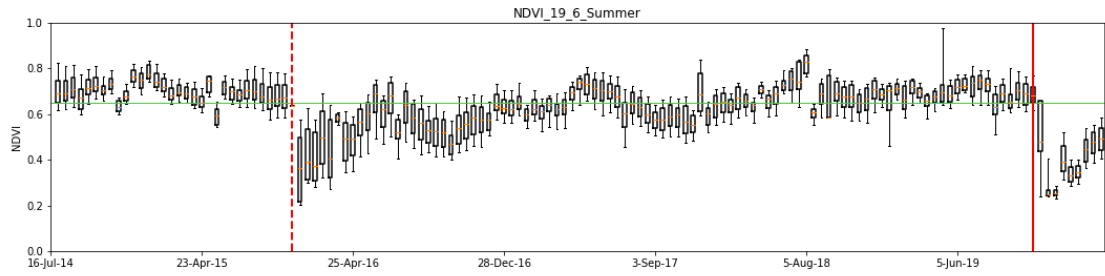


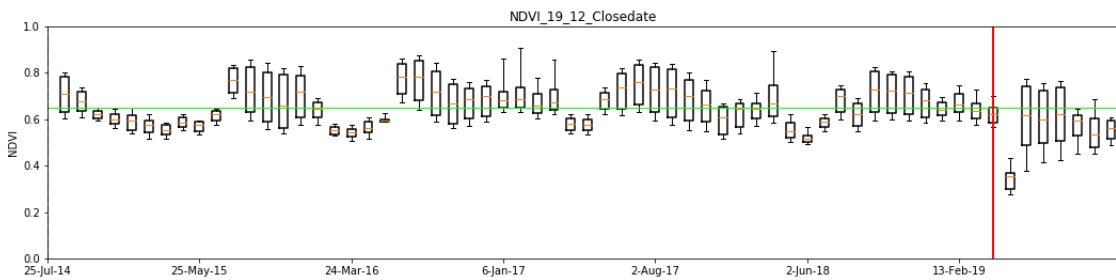
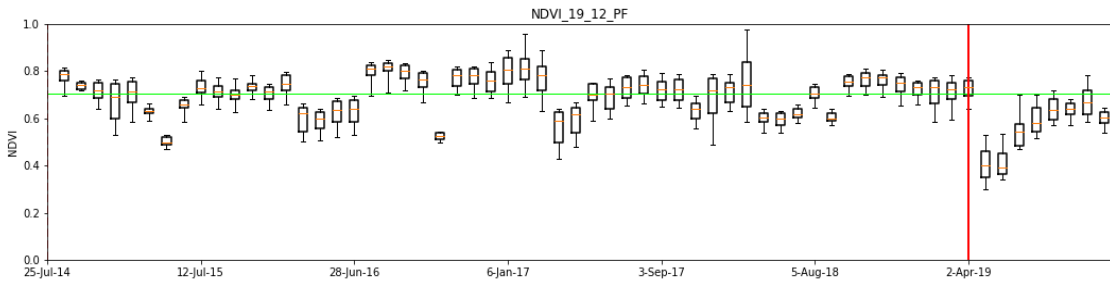
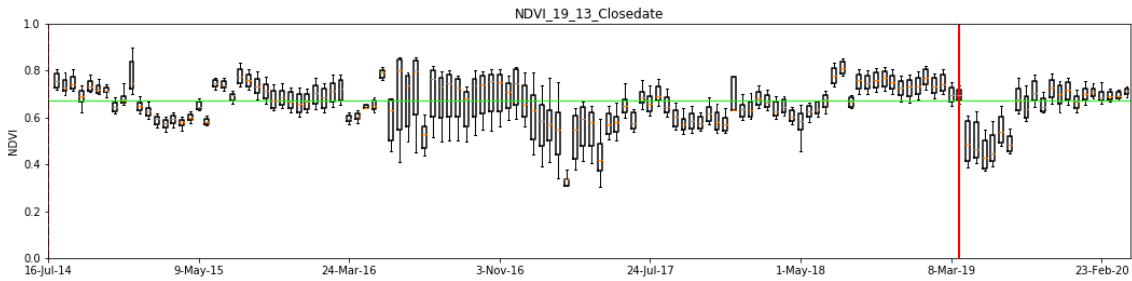
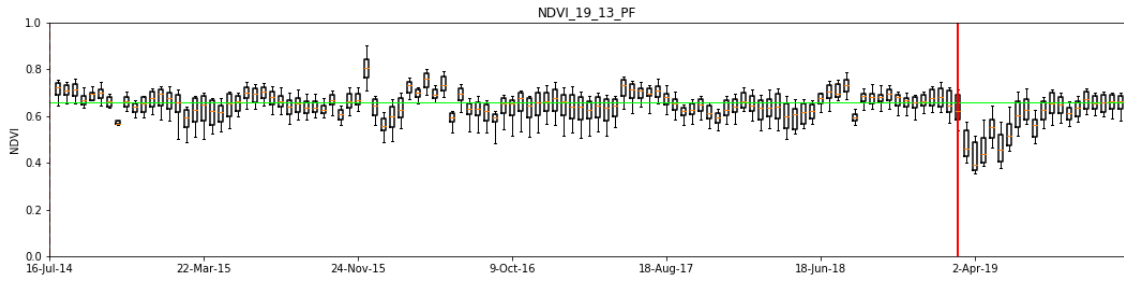
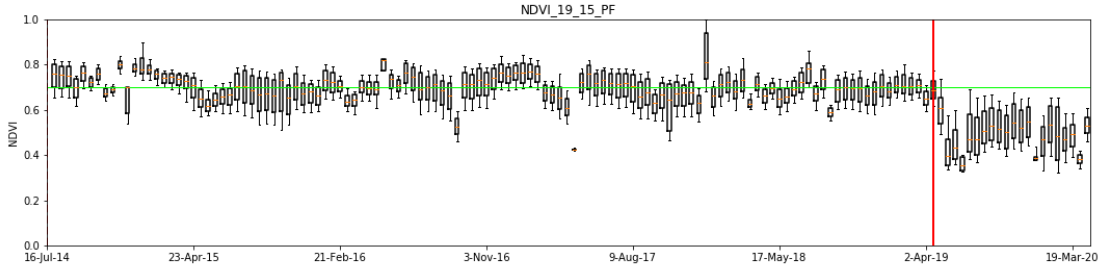
Winter Wildfires 2019_13

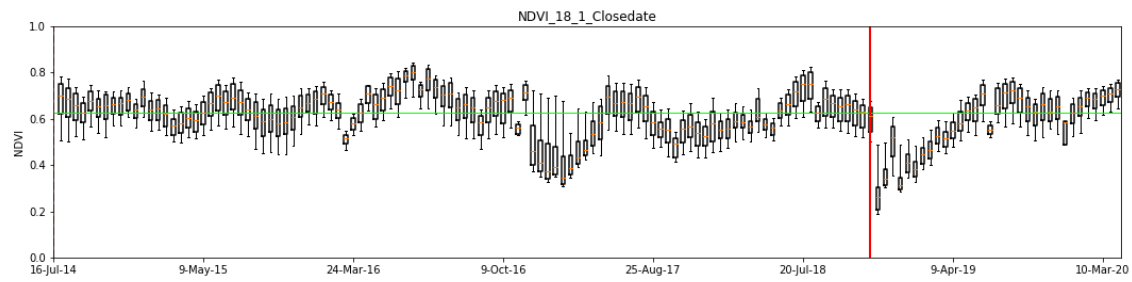
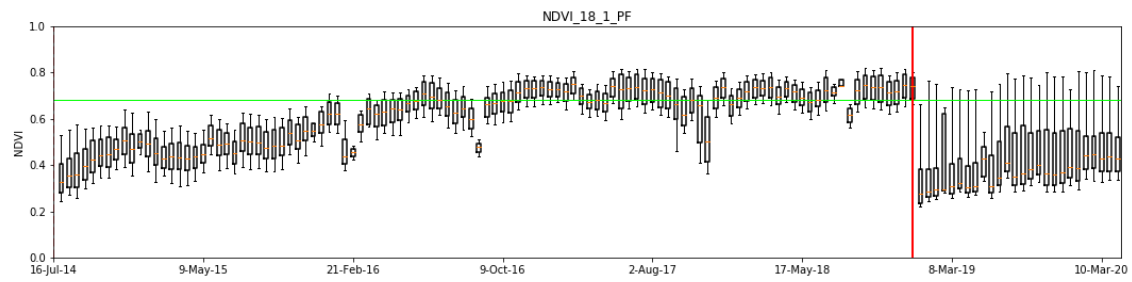
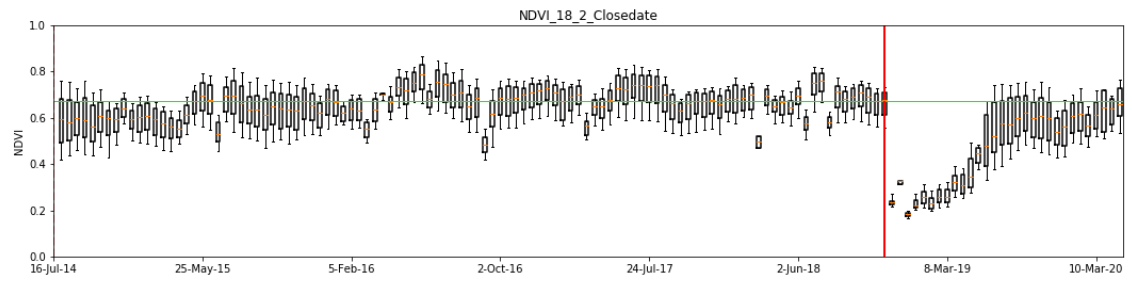
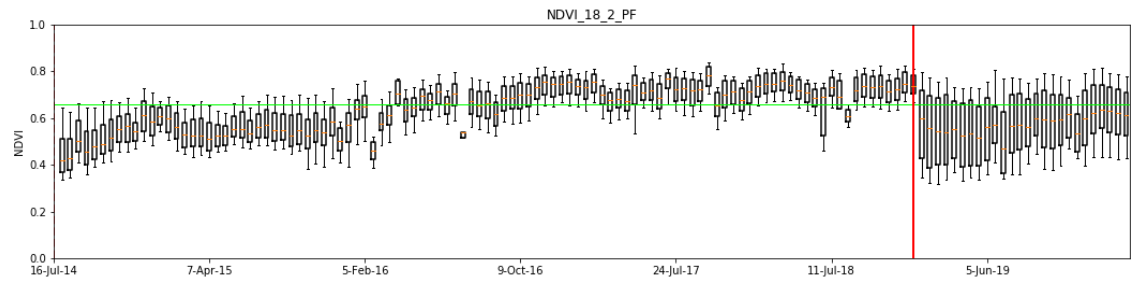
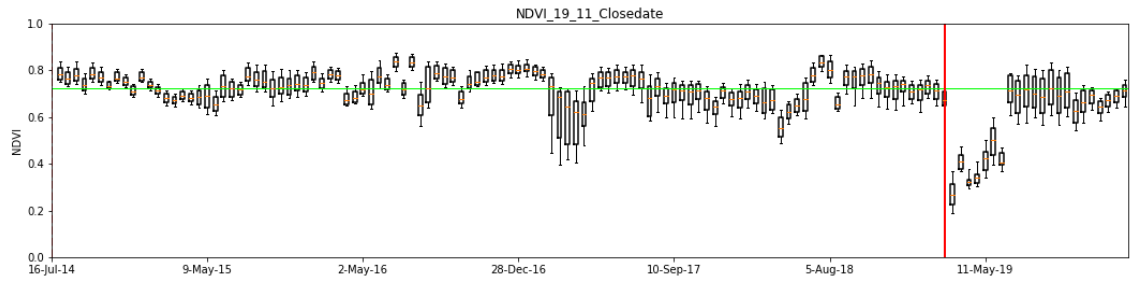
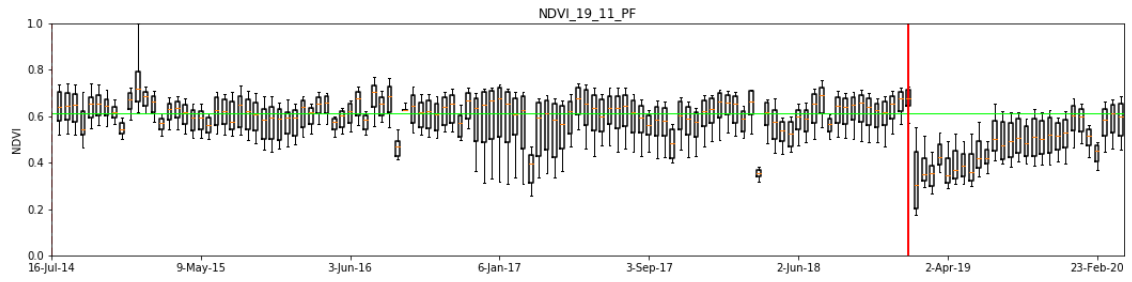


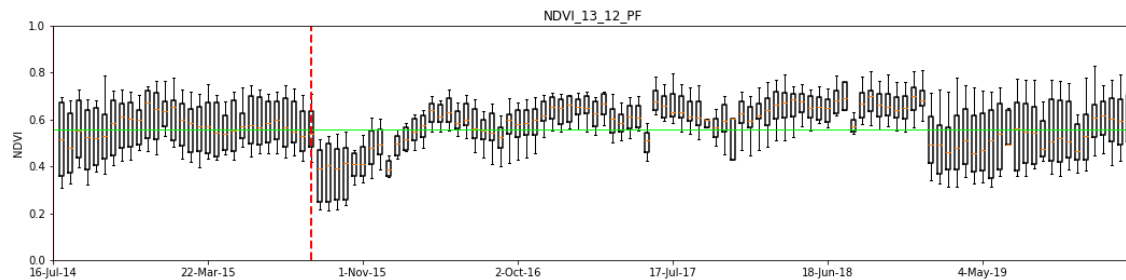
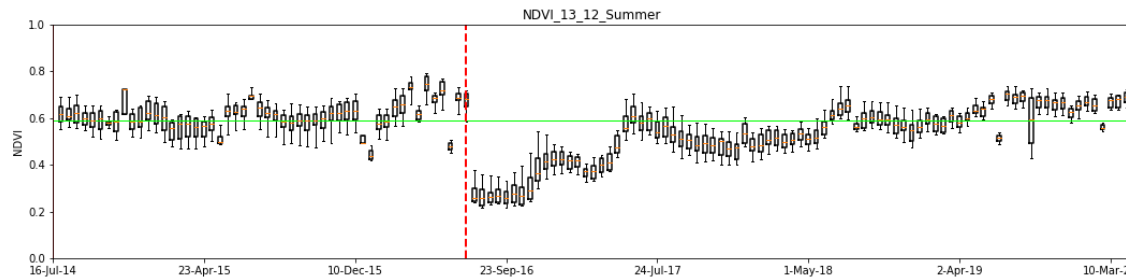
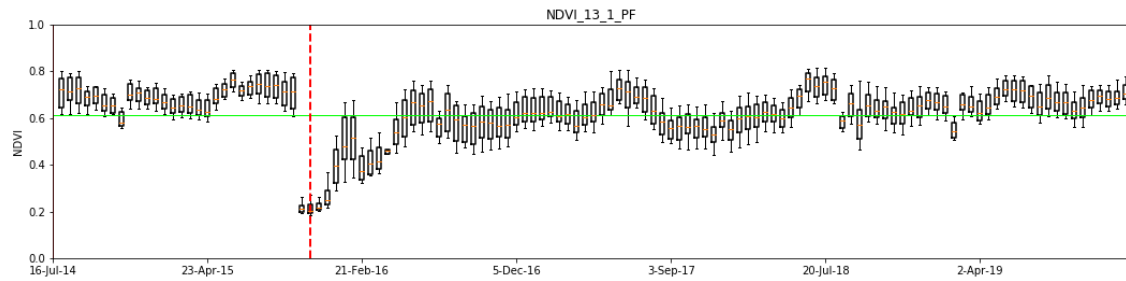
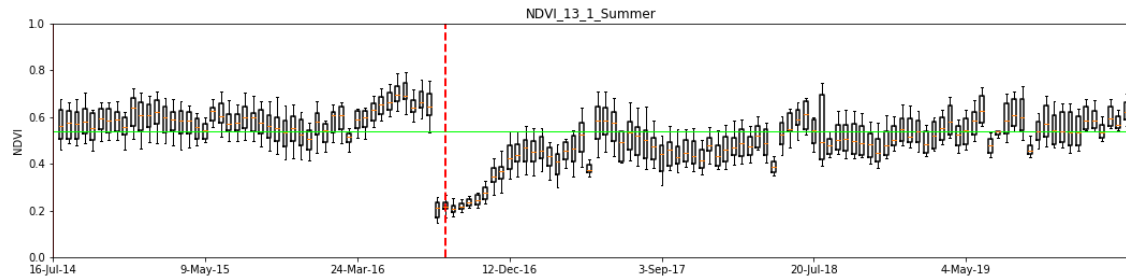
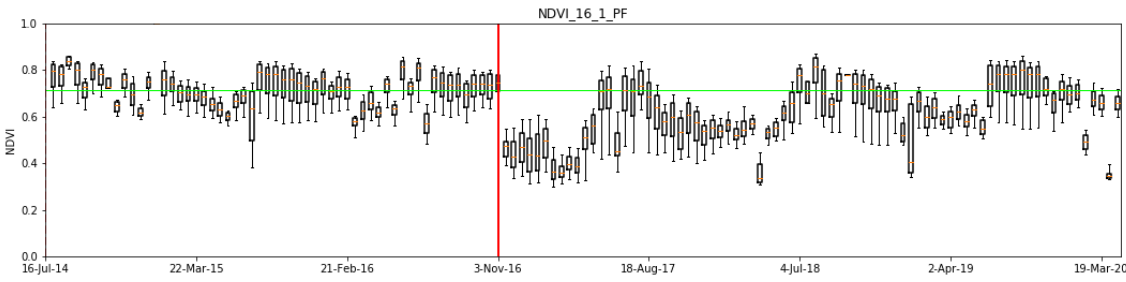
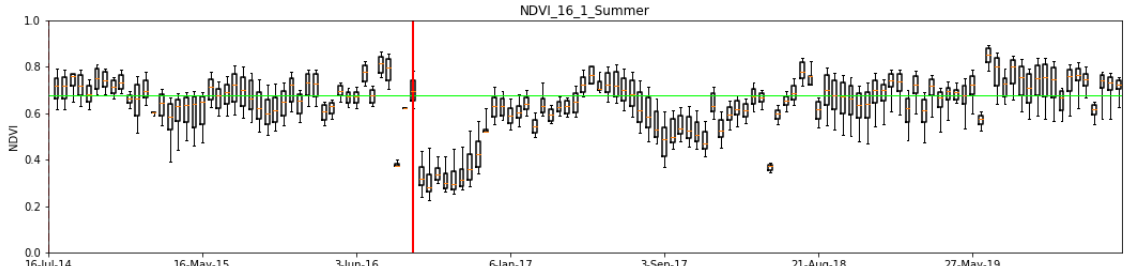
Appendix 3 – NDVI boxplot for each area analysed, where “closedate” is Winter/Autumn wildfire areas; “Summer” is Summer wildfires and “PF” is Prescribed Fires.











Appendix 4 – NBR boxplot for each area analysed, where “Closedate” is Winter/Autumn wildfire areas; “Summer” is Summer wildfires and “PF” is Prescribed Fires.

